Bolometers for infrared and millimeter waves

P. L. Richards

Citation: J. Appl. Phys. **76**, 1 (1994); doi: 10.1063/1.357128
View online: http://dx.doi.org/10.1063/1.357128
View Table of Contents: http://jap.aip.org/resource/1/JAPIAU/v76/i1
Published by the American Institute of Physics.

Bolometers for infrared and millimeter waves

P. L. Richards
Department of Physics, University of California, and Materials Sciences Division, Lawrence Berkeley Laboratory, University of California, Berkeley, California 94720

(Received 16 August 1993; accepted for publication 10 March 1994)

This review describes bolometric detectors for infrared and millimeter waves. The introduction sketches the history of modern bolometers, indicates how they fit into the more general class of thermal detectors, and describes the types of applications for which they are the optimum solution. Section I is a tutorial introduction to the elementary theories of bolometer response, of thermal radiation, and of bolometer noise. Important results are derived from the laws of thermal physics in the simplest possible way. The more rigorous theories of bolometer response and noise that are required for quantitative understanding and optimization are then summarized. This material is intended to provide the background required by workers who wish to choose the appropriate bolometer technology for a given measurement, or to evaluate a novel technology. Section II, then describes the various components of an efficient bolometer and gives details of the fabrication and performance of modern bolometers. This discussion focuses on composite bolometers with semiconducting thermometers for operation at and below liquid helium temperatures. The tradeoffs involved in using superconducting thermometers at low temperatures are discussed. Finally, a discussion is given of bolometers for operation at liquid nitrogen temperature which use the new high-T_c superconductors as thermometers.

TABLE OF CONTENTS

I. PRINCIPLES OF BOLOMETER OPERATION

A. Introduction

Infrared radiation was discovered by Herschel[1] using a mercury-glass thermometer to detect sunlight that had been dispersed by a prism. Thermal detectors have played an important role in the exploration and exploitation of infrared radiation to the present date. Both room-temperature and cooled thermal detectors have found widespread applications.

All thermal radiation detectors include an absorbing element with heat capacity C which converts the incident electromagnetic radiation to heat, and which is attached to a heat sink at temperature T_S via thermal conductance G. After the incident radiation power P is turned on, the temperature T_B of this absorbing element initially increases with time at rate $dT_B/dt=P/C$ and approaches the limiting value $T_B=T_S+P/G$ with the thermal time constant $\tau=C/G$. When the radiation is turned off, it relaxes back to T_S with the same τ. Thermal detectors are frequently used to give a periodic response to a signal which is modulated at a frequency $\omega\approx 1/\tau$. In a few cases they are used to detect pulsed signals or steady state radiation levels.

Thermal detectors differ in the means used to read out the temperature excursions in the radiation absorber. The following frequently used examples will illustrate the range of possibilities. In the radiation thermopile, the thermoelectric effect is used as the temperature readout. The output impedance of this thermometer is increased by using many thermocouples in series, the hot junctions on the absorber, and the cold junctions on the heat sink. In the Golay pneumatic detector, the heat absorbed in a thin metal film is transferred to a small volume of gas. The resulting pressure increase changes the angle of a mirror in an optical amplifier. In the pyroelectric detector, the absorbed heat increases the temperature of a material whose dielectric constant is a sensitive

 0021-8979/94/76(1)/1/24/$6.00

function of temperature. This pyroelectric material is contained in a voltage-biased capacitor which acts as a source of current proportional to the time rate of change of the dielectric constant. Both the Golay and the pyroelectric detector have been widely used in laboratory infrared spectrometers since the 1960s.

The bolometer, which was developed by Langley,[2] is a thermal infrared detector which employs an electrical resistance thermometer to measure the temperature of the radiation absorber. The popularity of bolometric infrared detectors arises, in part, from the fact that the temperature dependence of the resistivity of materials can be very large and has been widely studied. Consequently, it has been relatively easy to select materials to optimize bolometer designs for various applications. Several different bolometer architectures will be described in this review. For purposes of illustration, we will begin by describing the components of a typical composite bolometer and the properties that these components must have for efficient bolometer operation. The radiation absorber has a size appropriate to intercept the signal to be measured, a large absorptivity over the frequency range of interest, and a low heat capacity. The supporting substrate has a low heat capacity and large thermal conductivity, so that it remains isothermal during bolometer operation. The thermometer is thermally attached to the radiation absorber and/or the supporting substrate. It has low heat capacity, low electrical noise, and an adequate temperature dependence of its electrical resistance. The thermal link, which connects the thermally active portions of the bolometer to the heat sink has low heat capacity and an appropriate thermal conductance for the required application. The heat sink has a stable temperature appropriate for the application. The mechanical support for the thermally active portion of the bolometer has low heat capacity, low thermal conductance, and must be stiff enough that the mechanical resonant frequencies are higher than the operating frequency of the bolometer. Bolometers combine these various elements in various ways. In some bolometers, a single element is used for several functions. In composite bolometers, these functions are accomplished by separate elements so that they can be optimized independently.

Despite their long history, bolometric radiation detectors were little used in the 1950s. The room temperature thermal detectors, such as the Golay cell and the thermopile had advantages of sensitivity or operating convenience. Smith *et al.*[3] give an excellent review of the status of infrared measurements at this time. The advantages of operating thermal detectors in general and bolometers in particular at low temperatures were known. Early experiments had been carried out by Andrews *et al.*[4] using the temperature dependence of the resistance of a metal at the transition to the superconducting state as the thermometer. The specialized techniques required for such bolometers, however, were not generally available to the users of radiation detectors.

The modern history of infrared bolometers begins with the introduction of the carbon resistance bolometer by Boyle and Rogers.[5] At this time, carbon radio resistors were widely used by low temperature physicists as thermometers at liquid helium temperatures. Boyle and Rogers used the carbon resistor material both as the radiation absorber and the resistive thermometer. This device had a number of advantages over the Golay cell. It was relatively inexpensive and easy to fabricate. It benefited from the large reduction in heat capacity that occurs in solids at low temperatures. It was very convenient for use in experiments to measure the infrared properties of materials at low temperatures, since the detector could be placed inside the cryostat close to the sample under study. The technology required was immediately available to solid state physicists working at liquid helium temperatures. From the modern viewpoint, the carbon resistance bolometer had two major drawbacks. The heat capacity of the carbon resistance material was not as low as the crystalline materials employed later. More important, the resistor material has excess low frequency noise which limited bolometer sensitivity. The proprietary nature of this material hindered attempts to reduce the noise.

Shortly after this bolometer development, work began on the pyroelectric detector by Cooper[6] and Hadni[7] which has become the most widely used ambient temperature thermal infrared detector.

The next important step in bolometer development was the invention of a low temperature thermometer based on heavily doped and compensated germanium. Although this technology was not as available as the carbon resistor, the advantages of a well-known material with reproducible properties, high stability, and low noise led to its adoption for many low temperature experiments. The landmark paper by Low[8] showed how the germanium resistance thermometer could be used to make a superior bolometer. This development was rapidly applied to infrared astronomy at medium and long wavelengths as well as to laboratory infrared spectroscopy.

A further step in the development of modern bolometers came with improvements in the radiation absorbing element. The early superconducting bolometer of Andrews *et al.*[4] used a blackened metal foil attached to the Ta thermometer. Low's original bolometer was coated with black paint. Coron *et al.*[9] used a metal foil as the substrate for a black paint absorber. A small doped germanium thermometer was attached to read out the temperature. An improvement on this structure was made by Clarke *et al.*,[10] who substituted a thin low heat capacity dielectric substrate for the metal foil and used a low heat capacity bismuth film absorber in place of the black paint. This structure was quickly adapted for use with semiconductor thermometers. Variations of it are in current use at a variety of wavelengths where relatively large bolometers are required. A detailed investigation of the superconducting bolometer was carried out by Clarke *et al.*[10,11] This superconducting Al bolometer had very low heat capacity and reached the thermal fluctuation noise limits. Since the rapid change of resistance with temperature occurs only over a limited temperature range near the superconducting transition, however, it is necessary to use active control to maintain the bolometer in the operating range. Consequently, the required electronics were more complicated than those for the Ge bolometer.

The next step was the introduction of ion implantation to dope silicon appropriately for thermometers. Downey *et al.*[12] used silicon micromachining to produce a bolometer with a silicon thermometer implanted in a thin silicon substrate with silicon support legs. This bolometer had very little inherent low frequency noise. Bolometers based on this design concept are currently used both for infrared detectors and for x-ray calorimeters.

The use of thermometer material doped by neutron transmutation rather than melt doping is described by Lange *et al.*[13] The neutron technique produces relatively large quantities of very homogeneous thermometer material in a controlled way. This led to the availability of large numbers of small bolometer chips with ion implanted contacts, described by Haller *et al.*[14,15] which are used by many workers to assemble composite bolometers. Melt-doped Si chips with ion implanted contacts are also extensively used both as chip bolometers and as thermometers in composite structures as described by Moseley.[16] In addition to these major developments, the success of modern bolometers depends critically on many innovations by many persons which will be described in later parts of this review. Although efforts have been made to balance this discussion, it inevitably emphasizes work known to the author and work that is fully described in the scientific literature.

Bolometric detectors for infrared and millimeter wavelengths have a wide variety of applications to laboratory and astronomical measurements. Different applications have very different requirements for sensitivity, speed, saturation, power, etc. In order to achieve very high sensitivity under conditions of low background power loading, bolometers are operated at and below ^{4}He temperatures. Bolometers cooled with ^{3}He were introduced by Drew and Sievers[17] for laboratory far infrared spectroscopy and are now conventional in many astronomical applications. Bolometers are increasingly being developed for operation at 0.1 K and below using demagnetization or dilution refrigerators. Despite the success achieved, challenges remain to the developers of bolometric radiation detectors. Arrays of bolometers are required increasingly for astronomical applications, but there exists no monolithic technology suitable for large format two-dimensional arrays such as the photon detector arrays used at shorter infrared and visible wavelengths. Some applications would benefit from further reductions in the volume of material which is thermally active. Various superconducting bolometer applications are being currently explored to meet these goals. The discovery of the high-T_c oxide superconductors has led to the possibility of useful bolometric radiation detectors which use liquid nitrogen (LN) as a coolant. This application depends on the fact that high-T_c superconducting films are extremely sensitive thermometers over a narrow temperature range around the superconducting transition temperature.

Bolometers belong to the operational category of square law transducers; they give an output voltage (or current) which is proportional to the square of the signal amplitude, that is to the incident power. This category includes semiconductor and superconductor diodes, extrinsic and intrinsic photoconductors, and also photovoltaic diodes. All can be used either as direct detectors or as mixers for coherent heterodyne downconversion. In all such devices the responsivity falls for frequencies above some relaxation frequency $1/\tau$. Depending on the device physics, the developer can vary $1/\tau$ over some range within which the output voltage per unit absorbed signal power is proportional to $\tau^{1/2}$.

For most bolometers the obtainable values of $1/\tau$ are too small to make heterodyne downconverters with useful bandwidths. Consequently, bolometers are almost always used as direct detectors. One notable exception is the InSb hot electron bolometer developed by Kinch and Rollin.[18] In this device the electrons in degenerately doped n-type InSb are both the absorber and the thermometer. They absorb millimeter and submillimeter wavelengths close to the plasma frequency and reach internal thermal equilibrium at a temperature above that of the lattice. The electrical resistance decreases with increasing electron temperature because Rutherford scattering of electrons from ionized impurities decreases with increasing electron velocity. The relaxation rate set by the electron-phonon interaction and the electronic heat capacity is $1/\tau \approx 10^7$/s. Although no longer competitive either as a low frequency direct detector or as a mixer, this device was used very successfully by Phillips and Jefferts[19] for a time as a mixer in astronomical heterodyne receivers for near-millimeter wavelengths. It was possible to avoid the usual tradeoff between speed and responsivity in a thermal detector by an architecture that achieved efficient waveguide coupling with a very small thermally active volume (small numbers of carriers). Hot carrier effects in other systems, such as Nb films have also been suggested as mixers by Gershenzon *et al.*[20]

Direct detection receivers respond to the square of the small signal amplitude but can have wide bandwidths and large throughput. Heterodyne receivers respond to the product of the signal amplitude with a much larger local oscillator amplitude, but are subject to quantum noise and are limited to relatively narrow bandwidths by the intrinsic relaxation frequency or by the IF amplifiers used and to single mode throughput. The selection of an optimum approach for a given experiment depends on the required wavelength, bandwidth, and throughput as discussed by Richards and Greenberg.[21] For single mode throughput and 10% bandwidth, for example, direct detectors are indicated for wavelengths shorter than a few millimeters. For bandwidths of 10^{-5}, direct detectors are used for wavelengths shorter than ~ 10 μm.

Thermal detectors can be distinguished from photon detectors which are widely used for infrared detection. The distinction cannot be made on the basis of a measurable response to a single photon. Many bolometers meet this criterion for x rays, and most photon detectors fail to meet it in the infrared. In both kinds of device the energy entering as photons departs as heat to a heat sink after several energy transfer steps. The distinguishing characteristic is that in a thermal detector the excitations generated by the photons relax to a thermal distribution at an elevated temperature (in the thermometer) before they are detected. In the photon detector, the nonthermal distribution of excited electrons (e.g.,

in the conduction band) is detected before it relaxes (e.g., to the conduction band).

Semiconductor photon detectors have improved to the point that bolometers are not generally used for conditions in which well-developed photon detectors can be used. A few exceptions to this rule occur when there are special requirements such as very high quantum efficiency, very broad spectral range, very broad dynamic range, or very accurate calibration. The long wavelength limits to photon detectors depend both on the available operating temperature and the lack of suitable materials with small excitation energies. Photon detectors must be operated at a low enough temperature that the number of photogenerated carriers is much larger than the number of thermally generated carriers. Thus kT must be sufficiently below the excitation energy hc/λ_c, where λ_c is the cutoff wavelength. This is the fundamental reason why HgCdTe detectors operated at 77 K rapidly lose performance as the cutoff wavelength is extended beyond 10 μm. In this case, however, difficulties with the narrow gap material are also important. At longer infrared wavelengths, room temperature thermal devices such as the Golay or pyroelectric detectors, or slightly cooled thermoelectric detectors are widely used in applications where LHe is not available, but LN temperatures are acceptable. Such applications include most chemical laboratory infrared spectrometers and long term observations of the earth or nearly planets from long-lived space platforms.

Photoconductive photon detectors made from doped Si and Ge show good performance out to 100 μm and this cutoff is extended to ~200 μm in Ge:Ga by shifting the electronic band energies with uniaxial stress. The temperature required for low dark current approaches 1 K for operation at 200 μm. Although materials such as InSb and GaAs have smaller impurity excitation temperatures than Ge, they are not available in sufficient purity to make useful photon detectors. Consequently, thermal detectors such as bolometers are the only choice for sensitive direct detectors for far infrared wavelengths $\gtrsim$200 μm.

B. Elementary calculation of bolometer responsivity

A bolometer absorbs a radiant input power $P_0 + P_1 e^{i\omega_S t}$[W] which usually has a steady part P_0 and a time varying part of amplitude P_1 and frequency ω_S. The temperature of the bolometer consequently varies as $T_B = T_0 + T_1 e^{i\omega_S t}$[K]. (In this review, the SI units for important quantities will be given in square brackets.) The bolometer contains a resistive thermometer which is biased with a constant current I, so it produces time varying electrical heat which can be written to first order as $I^2R(T)=I^2[R(T_0) +(dR/dT)T_1 e^{i\omega_S t}]$[W]. The bolometer loses power $\bar{G}(T_B-T_S)$ to the heat sink through the thermal conductance $\bar{G}$. Since the thermal conductivity $\kappa(T)$ depends rapidly on T in some useful materials, it is sometimes helpful to define an average thermal conductance. For a wire of length l and cross sectional area A,

$$\bar{G}=\frac{(A/l)}{(T_S-T_0)}\int_{T_0}^{T_S}\kappa(T)dT \quad [\mathrm{W/K}]. \tag{1}$$

Equating the input power to the output power plus the power stored in the heat capacity C gives,

$$P_0+P_1e^{i\omega_S t}+I^2R(T_0)+I^2(dR/dT)T_1e^{i\omega_S t} =\bar{G}(T_0-T_S)+GT_1e^{i\omega_S t}+i\omega_S CT_1e^{i\omega_S t}. \tag{2}$$

Here G is the dynamic thermal conductance dP/dT at the temperature T_0. Equating the time independent terms gives the steady state heat flow equation that determines the average operating temperature T_0 of the bolometer,

$$P_0+I^2R(T_0)=\bar{G}(T_0-T_S). \tag{3}$$

Equating the time varying terms yields

$$P_1/T_1=G+i\omega_S C-I^2(dR/dT). \tag{4}$$

We define the (voltage) responsivity of a bolometer as the change in voltage drop per watt of absorbed signal power $S_A=V_1/P_1=I(dR/dT)T_1/P_1$. From Eq. (4) this can be written,

$$S_A=\frac{I(dR/dT)}{[G-I^2(dR/dT)+i\omega_S C]} \quad [\mathrm{V/W}]. \tag{5}$$

The responsivity of a bolometer is influenced by thermal feedback. The temperature rise $T_1=P_1/\bar{G}$ expected from an increase in radiant power P_1 is modified by the fact that R changes and, so the bias heating changes. This effect can be expressed as an effective thermal conductance $G_e=G-I^2(dR/dT)$. It is useful to introduce a parameter $\alpha=R^{-1}(dR/dT)$ [K^{-1}], evaluated at $T=T_0$, to characterize the thermometer. We can then write $G_e=G-I^2R\alpha$. For semiconducting bolometers which have negative α, $G_e>G$. For superconducting bolometers which have positive α, $G_e<G$. This thermal feedback also influences the time response of the bolometer. The measured thermal time constant is $\tau_e=C/G_e$. Using these definitions, the absorbed power responsivity can be written,

$$S_A=IR\alpha/G_e(1+i\omega_S\tau_e) \quad [\mathrm{V/W}], \tag{6}$$

which has Lorentzian form.

The choice made above to bias the bolometer with constant current is usually used because of the convenience and performance of voltage amplifiers. In practice, the bias current is obtained with a voltage source and a load resistor $R_L \gg R$. Given a sensitive current amplifier, a voltage bias would be an acceptable operational mode. There is a divergence in S_A called thermal runaway for a bolometer with $\alpha>0$ when the bias current is large enough that $G_e=0$. An analogous effect occurs for a voltage biased bolometer with $\alpha<0$.

In semiconducting thermometers, the resistance can depend on the applied voltage even at constant lattice temperature due to effects such as hot electrons, variable range hopping, or non-ohmic (Schottky diode) contacts. In low-T_c superconductors, the resistance depends on current through the magnetic field it generates. Although these nonthermal nonlinearities can be very important, there are many cases in which they are small enough that the simple theory of responsivity given here can be used.

C. Measurements of bolometer responsivity

One direct way to measure the absorbed power responsivity S_A is to attach a heater to the bolometer and thus convert it to an ac calorimeter. In practice, this is desirable only if the heater and its leads do not degrade the bolometer performance. This technique has been used in a superconducting bolometer with an independent heater by Clarke *et al.*,[11] in composite bolometers with metal leads where the metal film absorber was used as the heater by Lange *et al.*,[13] and also for monolithic Si x-ray bolometers which have a separate ion-implanted heater by McCammon *et al.*[22]

A more generally useful, but less accurate technique is to measure the response of the bolometer to changes in the electrical power dissipated in the thermometer. The responsivity obtained in this way, making use of the simple responsivity model described above assuming no nonthermal nonlinearities, is often called the electrical responsivity S_E. A convenient way to carry out this measurement is described by Jones.[23] First, the dc I-V curve of the bolometer is measured for a range of currents and voltages around the anticipated operating point. This I-V curve is nonlinear due to heating by the bias current. For a bolometer with $\alpha<0$, $V(I)$ is linear with slope R near $V=0$, has a broad maximum and then decreases slowly for larger values of I. [For a bolometer with $\alpha>0$, the $I(V)$ curve shows a similar dependence on V.] The second step is to measure $R=V/I$ and $Z=dV/dI$ from the I-V curve for a range of bias points and compute the dc electrical responsivity at each point from Jones' expression,

$$S_E=(Z-R)/2IR \quad [\mathrm{V/W}]. \tag{7}$$

For the special case of no optical power, this result can be derived by eliminating dT from the two expressions $dV=d(IR)=RdI+V\alpha dT$, and $dP=GdT=d(IV)=VdI+IdV$ and then solving for $Z=dV/dI=R(G+\alpha P)/(G-\alpha P)$. Writing Eq. (5) in the form $S_E=\alpha V/(G-\alpha P)$ and eliminating G yields Eq. (7).

Accurate values of Z are best obtained in practice by using an analog adder to combine a small low frequency alternating voltage with a steady bias voltage across the series combination of the load resistor and bolometer, and reading out the bolometer voltage through a dc amplifier and an ac lock-in amplifier. Care must be taken to obtain an accurate value of the responsivity near the origin because both the numerator and denominator of Eq. (7) approach zero. It is desirable to measure $V(I)$ for both positive and negative I. Deviations from inversion symmetry are an indication of non-ohmic contacts which should be eliminated. The use of symmetry to identify the origin cancels the effects of thermal emfs which can be significant for low temperature bolometers. Measurements of ac I-V curves can give information about nonthermal nonlinearities which are typically fast as described by Mather.[24]

The responsivity of a bolometer can depend on the steady infrared background power loading P_0 through a shift in the operating temperature which is determined by Eq. (3). Because G generally increases with temperature, and (for semiconductor thermometers) α decreases, the responsivity decreases rapidly as the bolometer is heated. This form of saturation is often seen when cold bandpass filters are changed. Some users monitor the steady bolometer voltage (resistance) to detect this effect. Corrections can be calculated for a well-characterized bolometer. Although the derivation of Eq. (7) assumes no background infrared power, it is a valid method to obtain S_E for any given background, if the I-V curve is measured with the same background power.

Another type of saturation occurs when the temperature excursion T_1 from the modulated signal power P_1 is large enough that the differential approximation is not valid. In some measurements, bolometers are designed to saturate on large signals and the nonlinearity is removed by calibration. In measurements such as conventional Fourier transform spectroscopy, linearity is of special importance. The response of a given bolometer can be linearized by increasing the bias until $I^2R>P_1$. However, this will not generally correspond to the optimum bolometer for the application. Mather[25] and Griffen and Holland[26] give general discussions of the influence of background power on bolometer performance.

The optical responsivity S of a bolometer is the product of the absorptivity η times the absorbed power responsivity $S=\eta S_A$. Direct measurements of S using a calibrated source are possible in principle. Since, however, it is often very difficult to directly characterize the efficiency of the optical elements that are used to couple infrared radiation into a bolometer, it is more usual to make direct responsivity measurements at the entrance of the cryostat or other convenient location in the optical system. A comparison of the directly measured system responsivity with the value of S_A obtained as discussed above is then used to deduce information about the efficiency of the filters, the coupling structures, and the absorber.

It is sometimes necessary to completely characterize an existing bolometer whose properties are not known. This can be done if apparatus is available that can eliminate background power and provide a heat sink temperature T_S that is known and variable. Values of $R(T)$ and thus of α can be obtained by measuring $V/I=dV/dI$ at the origin of the dc I-V curve as a function of T_S. The ac technique described above is particularly useful here. Given $R(T)$, $\tilde{G}=IV/(T-T_S)$ can be obtained directly from the I-V curve. Finally, knowledge of the heat capacity C can be obtained from measurements of the time constant τ_e. An approximate value of τ_e can be obtained by observing the bolometer voltage $V(t)$ on an oscilloscope after a step change in I. It is also possible to obtain $S_E(\omega)$ from Eq. (7) by measuring Z over a range of frequencies. Depending on the apparatus available, it is often more convenient to measure the frequency dependence of S with an uncalibrated light source and a variable-speed chopper.

D. Power and noise in blackbody radiation

Since bolometers are usually used to detect thermal radiation and are strongly influenced by thermal backgrounds, it is useful to summarize some aspects of thermal radiation that are not presented in convenient form in elementary textbooks.

It is usual to work with an optical system which limits the beam to an area A and a solid angle Ω, and has filters with transmittance $\tau(\nu)$, where ν is the optical frequency. The

power transmitted through such a system from a blackbody source with the Planck spectral brightness $B_\nu(\nu,T)$ can be written,

$$P=\int_0^\infty P_\nu d\nu=\int_0^\infty A\Omega\tau(\nu)B(\nu,T)d\nu \quad [\mathrm{W}]. \tag{8}$$

The throughput $A\Omega$[sr m^2] is an invariant in an optical system, as can easily be proved from geometrical optics or, more generally, by considering two otherwise isolated black radiators that view each other through the optical system. The second law of thermodynamics requires that the temperatures of the two radiators are the same in equilibrium, which follows from Eq. (8) only if $A\Omega$ looking into both ends of the optical system is the same.

When diffraction is important, the throughput depends on the frequency (or wavelength λ). The antenna theorem states that for a single spatial mode, or diffraction limited beam, the throughput is exactly $A\Omega=\lambda^2$. This principle is easily illustrated by using Fraunhoffer diffraction theory to compute the solid angle of divergence Ω of a plane wave after passing through a circular aperture of area A. A more general treatment can be given in terms of two-dimensional Fourier transforms. When the solid angle or the area is not uniformly illuminated, an equivalent (pillbox) solid angle (or area) must be used for exact results. Infrared telescopes often use throughputs somewhat larger than the diffraction limit. For a uniformly illuminated circular aperture, 84% of the energy from a point source appears in a throughput $A\Omega=3.7\lambda^2$. Spatially incoherent light can be thought of as being made up from many modes. The number of modes is $N=A\Omega/\lambda^2$ for one polarization. This picture is of some value for the intermediate case of partially coherent light (small N). Lamarre[27] has provided a rigorous treatment which is much more complicated

A standard result of thermal physics is that for a blackbody source (matched load) the power per mode is

$$P_\nu d\nu=h\nu d\nu[\exp(h\nu/kT)-1]^{-1} \quad [\mathrm{W}], \tag{9}$$

which approaches $kTd\nu$ for $h\nu\ll kT$. See, e.g., Kittel and Kroemer.[28] The power $P(\nu,T)d\nu$ in a multimode source is just the number of modes times the power per mode. This gives the Planck result for the spectral brightness of a blackbody,

$$B(\nu,T)d\nu=\frac{2h\nu^3 d\nu}{C^2[\exp(h\nu/kT)-1]} \quad [\mathrm{W/m^2\,sr}]. \tag{10}$$

Like more conventional derivations of the Planck law, this argument implicitly identifies the thermal equilibrium number $n=[\exp(h\nu/kT)-1]^{-1}$ of photons per standing wave mode in a box at temperature T with the number of photons per s per Hz of infrared bandwidth in a spatial mode propagating in free space. Once this identification is made, then we can use the textbook expression[28] for the thermal average variance in the number of photons per mode inside the box $\langle(\Delta n)^2\rangle=n+n^2$ to compute the fluctuations in the number of photons arriving each second from the free space beam. Note than when $h\nu/kT\gg1$, we have $n\ll1$ and the fluctuations obey Poisson statistics, $\langle(\Delta n)^2\rangle=n$. In this case, the photon arrival is random. When there are many photons per mode $n\gg1$ the photons arrive in bunches and $\langle(\Delta n)^2\rangle=n^2$.

Since a bolometer detects power, we are interested in the mean square energy fluctuation which can be written $h^2\nu^2\langle(\Delta n)^2\rangle$. If we now make the simple assumption that fluctuations in energy in different modes and in different infrared bandwidths are uncorrelated, then their mean square fluctuations are additive. Then the mean square fluctuation in the energy arriving in 1 s is $\int h^2\nu^2 2N(n+n^2)d\nu$. Since the audio bandwidth associated with a 1 s unweighted average is 1/2 Hz, the mean square noise power per unit post-detection bandwidth B referred to the absorbed power at the input is

$$\frac{P_N^2}{B}=2\int P_\nu h\nu\, d\nu+\int P_\nu^2 c^2\, d\nu/A\Omega\nu^2 \quad [\mathrm{W^2/Hz}], \tag{11}$$

where we have written $2Nnh\nu=P_\nu$, the spectral power absorbed in the bolometer and set $N=A\Omega\nu^2/c^2$. Note that Planck's constant h does not appear in the second term, which is a property of classical waves.

The first term in Eq. (11) can be obtained more directly. For Poisson statistics, the mean square fluctuation in the number of photons arriving in 1 s is just equal to the number of photons arriving $\langle(\Delta n)^2\rangle=P_\nu/h\nu$. If we multiply by $h^2\nu^2$ to obtain fluctuations in power and by $2B$ to convert a 1 s average to a bandwidth of B Hz, we obtain the first term in Eq. (11). This term has been verified experimentally in many experiments. The second term, by contrast, has not been measured unambiguously.

Although the form given in Eq. (11) appears frequently in the literature, including papers by van Vliet[29] and Mather,[24,25,30] there are theoretical arguments and indirect experimental data which show that it is not correct. The argument can be understood from the central limit theorem of probability theory. When the fluctuations from enough modes are combined, the resulting distribution should be Gaussian (of which Poisson statistics is a special case). Jakeman and Pike[31] and Lamarre,[27] for example, argue that the second term in Eq. (11) should have a factor $q=2A\Omega\Delta\nu T/\lambda^2$ in the denominator. Here, q is the number of modes of one polarization detected in the frequency band $\Delta\nu$ during the time T, which is a very large number for most bolometric systems. Jakeman, Oliver, and Pike[32] found experimental evidence for this averaging effect in the scattering of visible light from dielectric spheres. Although the full Eq. (11) with the factor q in the denominator will be retained in the rest of this review for completeness, it may prove that the second term can be neglected in almost all practical situations.

This discussion must now be generalized to treat real systems which have sources with emissivity ϵ, cold filters with transmissivity τ, and bolometers with absorptivity η. We will assume throughout this review that the bolometer is cold enough that fluctuations in the power emitted by the bolometer can be neglected. The number of photons per s per mode per Hz, which is $n=[\exp(h\nu/kT)-1]^{-1}$ for a blackbody becomes $n=\epsilon\tau\eta[\exp(h\nu/kT)-1]^{-1}$ inside the bolometer where the nonlinear processing takes place. For $T=300$

K and $\epsilon\tau\eta=1$, we get $n=1$ at $\lambda\sim100$ μm. For a more typical $\epsilon\tau\eta=0.1$, $n=1$ at $\lambda=1$ mm. Consequently, the first term in Eq. (11) typically dominates for infrared systems and the second term with $q=1$ would be important for millimeter wave systems. Although the two limits of photon noise are analogous to the Rayleigh–Jeans and Wien limits of the Planck theory, it is clear that the fundamental variable is n, the number of photons per second in one mode in one Hz of infrared bandwidth, not $h\nu/kT$.

A frequently used figure of merit is the noise equivalent power (NEP), which is defined as the incident signal power required to obtain a signal equal to the noise in a one Hz bandwidth ($P_S=P_N$). Note that the NEP is a measure of S/N, not just noise. If we refer the NEP to the inside of the detector, then the signal power *absorbed in the detector* that is required is just $\mathrm{NEP}_A=P_N B^{-1/2}$ from Eq. (11). It is more conventional, however, to refer the NEP to the detector input. The signal power *incident on the detector* required to produce S/N=1 is then

$$(\mathrm{NEP})^2=\frac{2}{\eta^2}\int P_\nu h\nu\, d\nu + \frac{1}{q\eta^2}\int P_\nu^2 c^2\, d\nu/A\Omega\nu^2 \quad [\mathrm{W^2/Hz}], \qquad (12)$$

where P_ν, as defined above, is the power absorbed in the detector. This expression is used to calculate the photon noise contribution to the detector noise for an existing system when the throughput $A\Omega$ is known from the optical geometry and the absorbed power spectral density can be estimated from the filter bands, the bolometer output and the absorbed power responsivity $S_A\approx S_E$. Although originally introduced to describe photoconductors, the term BLIP is often used to describe any detector whose noise in a given application comes only from photon fluctuations in the infrared background.

E. Photon noise calculations

Calculations of background power and photon noise expected from thermal sources are important in the design of bolometric detector systems. From Eq. (8) the absorbed power in a band of frequencies from ν_1 to ν_2 is

$$P=(2k^4/c^2h^3)T^4A\Omega\epsilon\tau\eta\int_{x_1}^{x_2}x^3\, dx/(\exp x-1) \quad [\mathrm{W}], \qquad (13)$$

where $x=h\nu/kT$ and $2k^4/c^2h^3=2.782\times10^{-13}$ in SI units. An analogous expression for photon noise limited NEP referred to the detector input is obtained by writing the absorbed power spectral density in Eq. (12) as $P_\nu=\epsilon\tau\eta A\Omega B(\nu,T)$. The full expression can be written as

$$(\mathrm{NEP})^2=\left(\frac{4k^5}{c^2h^3}\right)\frac{T^5A\Omega\epsilon\tau}{\eta}\left(\int_{x_1}^{x_2}\frac{x^4\, dx}{(\exp x-1)} + \frac{\epsilon\tau\eta}{q}\int_{x_1}^{x_2}\frac{x^4\, dx}{(\exp x-1)^2}\right) \quad [\mathrm{W^2/Hz}], \qquad (14)$$

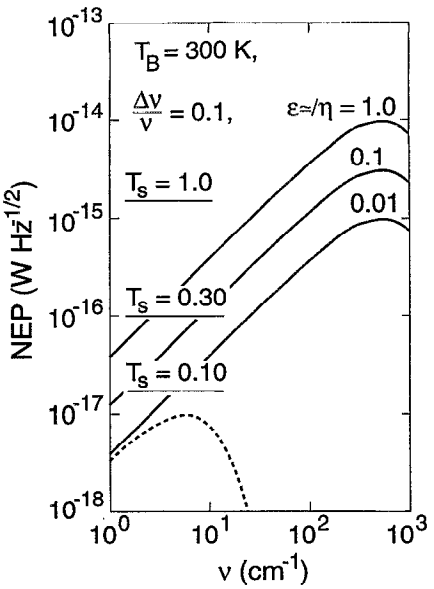

FIG. 1. Photon noise limited NEP calculated from the first term in Eq. (14) for a diffraction limited throughput $A\Omega=\lambda^2$, and a bandwidth $\Delta\nu/\nu=0.1$. The curves are for a 300 K source with $\epsilon\tau/\eta=1.0$, 0.1, and 0.01 and for a 3 K source with $\epsilon\tau/\eta=1.0$. Note that these curves can be scaled as $(A\Omega/\lambda^2)^{1/2}(\epsilon\tau/\eta)^{1/2}$. Horizontal lines are used to show the values of NEP achieved by composite bolometers in negligible background for several values of T_S. These values of NEP are referred to the detector input. To convert to the system input, divide the NEP by the system transmittance $\tau^{1/2}$.

where $4k^5/c^2h^3=7.684\times10^{-36}$ in SI units. A computer program that calculates Eqs. (13) and (14) is a useful tool. When there are several contributions to photon noise, it is necessary to compute the total absorbed power spectral density. Because of the term in P_ν^2, it is not correct to combine values of NEP calculated separately for each source. Illustrations of Eq. (14) are given in Fig. 1 for parameters appropriate for astronomical systems.

Finally, it is sometimes useful to compute the signal power *incident on the apparatus* required to produce S/N=1. This photon noise limited system $\mathrm{NEP}_S=\mathrm{NEP}/\tau$ varies as $\tau^{1/2}$ in the high frequency limit and is independent of τ in the low frequency limit.

Expressions related to Eq. (14) are seen in the literature for the NEP or the noise equivalent photon rate NEN of photon detectors such as photoconductors and photovoltaic diodes. The derivation differs from that given above in that the mean square fluctuation in the photon rate $\langle(\Delta n)^2\rangle$ for different infrared bandwidths are added directly and not multiplied by $(h\nu)^2$ to obtain energy fluctuations before adding as was done above for a bolometer.

F. Sources of noise in bolometers

The Nyquist noise in a resistor in thermal equilibrium at temperature T can be calculated as a special case of the foregoing arguments. The blackbody power radiated by a matched resistor into a transmission line which can only transmit a single mode with a single polarization is given by Eq. (9), which is just the Planck expression (10) with the

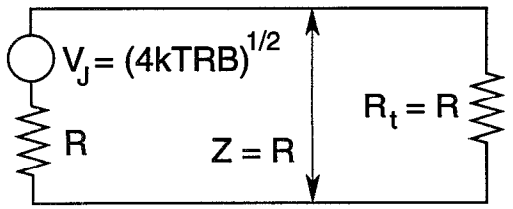

FIG. 2. Johnson noise source with resistance R matched to a two wire transmission line with characteristic impedance R and to a termination resistance R. The power flow to the right is kTB.

number of modes $2N$ set equal to unity. For audio frequencies, $h\nu/kT \ll 1$, and for a bandwidth $d\nu = B$, the power spectral density is flat, $P_\nu d\nu = kTB$.

For purposes of calculation it is convenient to replace this noisy resistor by an equivalent circuit consisting of an ideal noise-free resistor R in series with a Johnson noise voltage generator with rms voltage fluctuations,

$$V_N = (4kTRB)^{1/2} \quad [\mathrm{V}]. \tag{15}$$

This representation can be justified by coupling the ideal resistor with its voltage noise generator to a two wire transmission line with characteristic impedance $Z = R$, which is terminated by a matched resistance $R_t = R$ that is assumed to be at $T = 0$, as is shown in Fig. 2. The power dissipated in R_t by the noise current I_N driven around the loop from the Johnson noise generator is $I_N^2 R_t = V_N^2 R/(R + R_t)^2 = kTB$. This is just the result expected for a blackbody at temperature T radiating to a blackbody at $T = 0$ through a throughput limiter that transmits only one mode.

The detector responsivity S can be used to refer Johnson noise in the thermometer resistance R to the detector input. Expressed as a contribution to the NEP, we have

$$(\mathrm{NEP})^2 = 4kTR/|S|^2 \quad [\mathrm{W^2/Hz}], \tag{16}$$

where the modulus squared of S is used because the phase is *not* important. In principle, the Johnson noise in the load resistor must also be considered. It is usually made negligible by the use of a large load resistance $R_L \gg R$ cooled to the temperature T_S, of the heat sink.

Fluctuations in the energy of a bolometer produce a noise that is variously called energy fluctuation noise, thermal fluctuation noise, G noise, or phonon noise. The thermal circuit of a bolometer consists of a system with heat capacity C connected via a thermal conductance G to a heat sink at T_S. The thermal equilibrium mean square energy fluctuations in this system are calculated in standard thermal physics texts such as Kittel and Kroemer[28] to be $\langle (\Delta u)^2 \rangle = kT_S^2 C$. In a bolometer, there is an electrical resistance thermometer which reads out a temperature fluctuation $\Delta T = \Delta u/C$. The mean square temperature fluctuation can be written as an integral over a temperature spectral intensity $S_T(\nu)$ such that

$$\langle (\Delta T)^2 \rangle = kT^2/C = \int_0^\infty S_T(\omega) d\omega/2\pi \quad [\mathrm{K^2}]. \tag{17}$$

Physically, this noise arises from the passage of quantized carriers of energy (phonons or electrons, or even photons) through the thermal conductance, which drive the bolometer

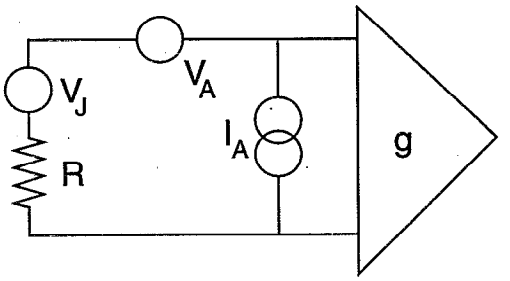

FIG. 3. Equivalent noise circuit for a bolometer of resistance R attached to an amplifier of gain g. Johnson noise in the bolometer is given by V_J. Current and voltage noise in the amplifier by I_A and V_A, respectively.

with white noise fluctuations with power spectral intensity S_P. We use the thermal equilibrium form of Eq. (4) with no thermal feedback to relate S_P to the temperature spectral intensity $S_T = S_P/(G^2 + \omega_S^2 C^2)$. From Eq. (17), we have $S_P = 2kT^2 G/\pi$ [W^2/rad] or

$$(\mathrm{NEP})^2 = 4kT^2 G \quad [\mathrm{W^2/Hz}]. \tag{18}$$

Like the photon noise, this NEP, which is referred to the bolometer input, is independent of the measurement frequency. In both cases, of course, the voltage noise at the bolometer output falls for $\omega\tau > 1$ because of the frequency dependence of the responsivity.

Excess low frequency noise, often called $1/f$ noise, has been a problem in bolometers. With improvements in materials and electrical contacts, electrical sources of $1/f$ noise in bolometers have become less important. In some cases the excess noise in an isothermal bolometer is proportional to the bias current I, so arises from resistance fluctuations which can be written as a spectral intensity S_R. In this case

$$(\mathrm{NEP})^2 = I^2 S_R/|S|^2 \quad [\mathrm{W^2/Hz}]. \tag{19}$$

Here the bolometer responsivity has been used to refer the voltage noise in the output to an effective power noise in the input in the usual way.

Low frequency noise due to changes in the temperature T_S of the heat sink is often important and is little discussed. This contribution to the NEP can be written

$$(\mathrm{NEP})^2 = G^2 S_T/\eta^2 \quad [\mathrm{W^2/Hz}], \tag{20}$$

where S_T is the spectral intensity of fluctuation in the temperature of the heat sink. Slow drifts can be reduced by active temperature regulation. Fast fluctuations such as noise due to boiling of cryogens in the signal bandwidth can be reduced by a passive low pass filter consisting of a heat capacity and a thermal link with a speed of response G/C that is small compared with ω_S.

Noise in the first stage of amplification can be important in bolometer systems. High impedance bolometers are generally used with JFET amplifiers whose noise can be represented by an equivalent circuit consisting of an ideal noise free amplifier with infinite input impedance plus two noise generators as is shown in Fig. 3. There is a rms current noise generator I_A in parallel with the input which represents shot noise in the diode leakage current. It is generally frequency independent, but increases with temperature. There is also a

rms voltage noise generator V_A in series with the input which varies as $1/f$ at typical bolometer operating frequencies. The equivalent noise circuit is understood to include a signal source resistance R (the bolometer) with its Johnson noise generator $V_J=(4kTR)^{1/2}$. Since the mean square fluctuations from uncorrelated sources can be added, the square of the voltage output noise for an amplifier with gain g can be written $g^2(V_A^2+I_A^2R^2+4kTR)$. If we divide by g^2 to refer to the amplifier input and by $|S|^2$ to refer to the bolometer input, then the combination of amplifier noise and thermometer Johnson noise can be written,

$$(\mathrm{NEP})^2=(V_A^2+I_A^2R^2+4kTR)/|S|^2 \quad [\mathrm{W^2/Hz}]. \tag{21}$$

The noise temperature T_N is a useful figure of merit for an amplifier. It is the physical temperature of a source resistor whose Johnson noise power just equals the amplifier noise,

$$T_N=(V_A^2+I_A^2R^2)/4Rk \quad [\mathrm{K}]. \tag{22}$$

For amplifier noise to be unimportant for a resistive transducer, such as a bolometer, it is sufficient to have T_N less than the operating temperature of the transducer. Note that T_N depends on the value of the source resistance R and has a minimum value when $R=V_A/I_A$. Semiconductor bolometers are designed to have a resistance R close to V_N/I_N which is $0.5<R<20$ MΩ for useful FET amplifiers. The best FET amplifiers have minimum $T_N\approx 0.1$ K for frequencies >10 Hz.

Following Low and Hoffman,[33] it is useful to add the sum of the squares of the values of NEP which arise from separate uncorrelated noise sources to obtain an overall NEP for power *incident* on the bolometer. In most cases the noise is dominated by photon, energy fluctuation, Johnson or amplifier noise, so

$$(\mathrm{NEP})^2=(\mathrm{NEP})^2_{\mathrm{photon}}+4kT^2G/\eta^2 + (4kTR+V_A^2+I_A^2R)/|S|^2 \quad [\mathrm{W^2/Hz}]. \tag{23}$$

An ideal BLIP detector is limited by the first term only. Bolometers are often limited by the second (energy fluctuation noise) term. The Johnson noise and amplifier noise terms can be made negligible by an adequately large responsivity S. Values of S larger than needed to meet this condition are not generally useful. It is often desirable to adjust $\alpha=R^{-1}(dR/dT)$ for the optimum trade-off between responsivity and dynamic range, while keeping R close to the optimum noise resistance of an appropriate amplifier.

In many cases, the NEP of a bolometer of area A, like that in other infrared detectors, scales at least approximately as $A^{1/2}$. The photon noise in Eq. (14) has this property. If the thermal time constant is held fixed, and the bolometer heat capacity is proportional to area then $G\propto A$ and $S\propto A^{-1}$, then all of the major contributions to the NEP in Eq. (23) scale as $\mathrm{NEP}\propto A^{1/2}$. Under these circumstances, the specific detectivity $D^*=A^{1/2}/\mathrm{NEP}$ $[\mathrm{cm\,Hz^{-1/2}\,W^{-1}}]$ is a useful figure of merit.

G. Nonequilibrium noise theory

In the previous section we have sketched the derivation of the simple thermal equilibrium theories of the various contributions to the noise in bolometers. These expressions are very useful for obtaining an intuitive understanding of bolometer operation and optimization, and for simple semiquantitative calculations. It is important to understand, however, that since a bolometer is not operated in thermal equilibrium, they are not correct in principle. They are all modified by the thermal feedback discussed in Sec. I A. A summary of the rigorous theories of bolometer responsivity, noise, and optimization appears in a series of papers by Mather.[24,25,30,34] Except, possibly, for the absence of the factor q, these papers are authoritative. The method of presentation, however, assumes that the reader has a working knowledge of the various approximate results which have been described above. Mather finds that thermal feedback in a typical semiconducting bolometer with $\alpha<0$ reduces the Johnson noise contribution to the NEP by as much as 60% and that the NEP depends on the time constant C/G, not the effective time constant $\tau_e=C/G_e$. Depending on the method of operation and the temperature dependence of the thermal conductance, the energy fluctuation contribution to the NEP is reduced by as much as 30% below $4kT^2G$. These expressions have been extended to include the effects of the nonthermal nonlinearities observed in semiconducting bolometers.[24] An illustration of the correction required to the equilibrium theory[13] is shown in Fig. 4.

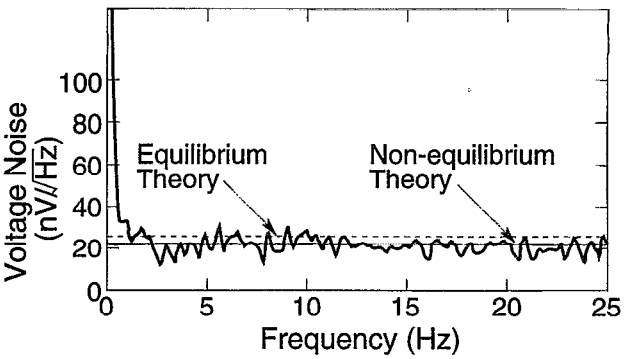

FIG. 4. Noise spectrum of a low-background composite bolometer at its optimum bias point. The dashed line indicates the noise level $V_n^2=4kT^2G|S|^2+4kTR$ expected from thermal equilibrium bolometer theory. The solid line indicates the noise level predicted by the nonequilibrium theory of bolometer noise for $\nu\gtrsim(2\pi\tau)^{-1}=8$ Hz. For frequencies $\nu\lesssim(2\pi\tau)^{-1}$, the nonequilibrium theory predicts a further decrease in the noise. For this bolometer the effect is of order 10% which may just be visible in the data.

H. Optimization of bolometric detector systems

Optimization of a bolometer for a given task, that is, for a measurement with a given throughput, bandwidth, heat sink temperature, background brightness, and modulation frequency is not an easy task. A more global optimization of an entire experiment is even more complicated. Some general comments may be helpful.

Large signal throughput is desirable to maximize signal power which is proportional to $A\Omega$. There are, however, obvious constraints. These include the size and beam collimation requirements of typical samples for laboratory studies, and the angular resolution requirements and optical size con-

straints for measurements of extended astronomical sources. The throughput for diffraction limited imaging is set by the wavelength. Once the throughput is large enough that the bolometer is limited by photon noise, the signal-to-noise ratio of an optimized bolometer will vary only as $(A\Omega)^{1/2}$. The same is true for an energy fluctuation noise limited bolometer if G is increased in proportion to area.

The choice of a signal modulation frequency ω_S is a trade-off between several factors. Fast modulation can sometimes be beneficial in avoiding sources of $1/f$ noise which occur in both the signal and reference phases of the modulation. Examples are sky noise from an infrared telescope which chops on and off the source, and $1/f$ noise from the bolometer. However, fast modulation can be mechanically difficult and the required speed of response can increase the NEP of an optimized bolometer for a low background measurement.

Cooled apertures and filters should be used to minimize sources of background power outside the signal throughput or signal spectral band. Cooled (or efficient) optics can reduce in-band backgrounds. Once the power P_0 on the detector is known, a decision must be made about the heat sink temperature. Typical values are T_S=77, 4.2, 1.2, 0.3, and 0.1 K, depending on the refrigeration system used.

An approximate calculation can be used to show that energy fluctuation noise can be made less than photon noise if T_S is chosen to be small enough. As a first approximation we choose the thermal conductance required to operate the bolometer with a typical value of the temperature rise at $(T_B-T_S)/T_S=0.5$. In terms of the absorbed power P we obtain $G=2P/T_S$ from Eq. (3). The energy fluctuation noise in this bolometer is $(\mathrm{NEP})^2=4kT_S^2G=8kT_SP$ from Eq. (18). The photon noise from the first term in Eq. (11) is $(\mathrm{NEP})^2=2Ph\nu$. The condition for a photon noise limited infrared bolometer is thus $h\nu\gtrsim 4kT_S$, which corresponds to $T_S\lesssim 3$ K at 1 mm wavelength and 30 K at 100 μm. For a millimeter wave bolometer with $q=1$, the second term in Eq. (11) is $(\mathrm{NEP})^2\approx P^2/Nd\nu$ (assuming that P arrives in N modes) so this condition becomes $P\gtrsim 8NkT_Sd\nu$. Thus the millimeter wave bolometer can be photon noise limited if $P\gtrsim$four times the power $2\tau\eta NkT_Sd\nu$ which would be received if the N modes were filled by a Rayleigh–Jeans source at the sink temperature T_S through an optical efficiency τ and absorptivity η. These are not difficult criteria for low temperature bolometers. The rigorous theory of bolometer optimization by Mather[25] calculates the optimum value for the temperature rise $(T_B-T_S)/T_S$ and so gives slightly different numerical factors from the approximate estimate presented here.

The choice of T_S should be based on requirements of sensitivity, operating convenience, and available bolometer technology. The various contributions to the bolometer NEP depend differently on T_S. The photon noise is independent of T_S as long as objects at T_S do not produce significant background. The dependence of the other contributions must be worked out case by case. Energy fluctuation noise, for example, varies as $TG^{1/2}$ from Eq. (18). When G is selected to maintain a given $(T_B-T_S)/T_S$ in the presence of a fixed P, then the $\mathrm{NEP}\propto T_S^{1/2}$. When it is chosen to maintain a given τ_e, then the $\mathrm{NEP}\propto T_S^{5/2}$. The choice of T_S can be driven by the need for large enough responsivity that Johnson noise and amplifier noise are negligible.

The area of a bolometer must be large enough to accept the signal throughput. The heat capacity should be small enough that its speed G/C is adequate for the application. This condition is usually easily met at high backgrounds and low temperatures but is often harder at low backgrounds and high temperatures. It is usually important to minimize the heat capacity per unit area and maximize the acceptance solid angle of low background bolometers. If the minimum possible heat capacity is large enough that $\omega_SC/G\gtrsim 1$, then it may be necessary to increase G above the value required to keep the bolometer cold. However, there is usually no absolute requirement for $\omega_SC/G\gtrsim 1$. The best choice for G is often that which minimizes the NEP for a given signal frequency ω_S. This is accomplished by selecting a value of G which makes the energy fluctuation noise equal to the combination of Johnson and amplifier noise. This condition may occur for $\omega\tau>1$. Energy fluctuation noise depends on G explicitly. Johnson and amplifier noise depend on G through the responsivity as given in Eq. (6).

A number of exceptions exist to the general statements made here about bolometer optimization. In experiments that must resolve signal pulses, there can be an absolute requirement for a small value of τ_e. Alternatively, Fourier transform spectroscopy is a technique that reduces the effects of detector noise, but requires linearity and a wide dynamic range. For an early treatment of the issues of bolometer optimization see Coron.[35] More modern discussions are given by Mather.[24] Bolometer theory has been organized in a form useful for computer optimization by Griffen and Holland.[26]

II. EXAMPLES OF USEFUL BOLOMETERS

Our ability to produce an optimized bolometer for a given measurement is often limited by the properties of available materials. The second part of this review describes the materials, architectures, and techniques which have proved useful in a variety of applications. This material is organized primarily by thermometric material and then by bolometer architecture and operating temperature. It includes references to work of historical significance as well as to current practice. Much detailed information about bolometer design and function is described in the context of real bolometers reported in the literature. This organization has the advantage of discussing concrete examples but the disadvantage that a reader interested, for example, in high-T_c superconducting bolometers should still read the sections on semiconductor bolometers to obtain a balanced overview.

A. Semiconductor thermometers

The temperature dependence of the resistance of a doped semiconductor, usually Si or Ge, is the most widely used thermometer for bolometers operated at or below LHe temperatures. Thermometer materials must be heavily doped, since the resistance of intrinsic or lightly doped extrinsic materials is inconveniently large at low temperatures. When semiconductors are doped close to the metal-insulator transition with a majority impurity and a compensating minority

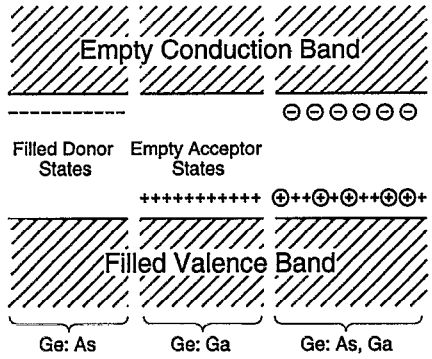

FIG. 5. Schematic representation at low temperature of electronic impurity states in Ge:As, Ge:Ga, and compensated Ge doped with a majority impurity Ga and a minority impurity As. Ionized (neutralized) impurity states are shown circled. In the compensated material, electrons from the donors fill some of the acceptor states. In the presence of an electric field, these electrons can hop to neighboring empty acceptor states.

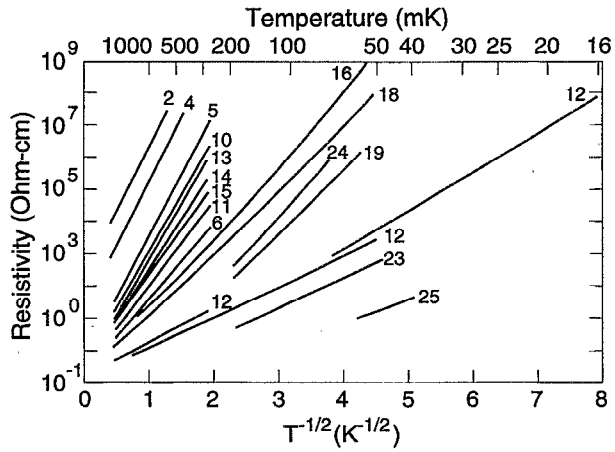

FIG. 6. Log of resistivity plotted as a function of $T^{-1/2}$ for 25 samples of NTD-Ge. The neutron fluence in units of 10^{18} cm^{-2} is 0.15 in sample 2, 1.24 in sample 13, 2.61 in sample 18, and 4.20 in sample 25. The straight lines show excellent agreement with the temperature dependence expected for hopping conductivity. This plot was adapted from one supplied by Beeman.

impurity, conduction is by variable range hopping as described by Efros and Shklovskii.[36] This process is illustrated for gallium doped germanium compensated with As in Fig. 5. Because of the large acceptor concentration N_A used, the impurity states interact, and the Stark effect gives a random variation in acceptor energy. Electrons hop with the absorption or emission of phonons giving a temperature dependent resistance of the form $R=R_0\exp(A/T)^{1/2}$, so that $\alpha=R^{-1}(dR/dT)=1/2(A/T^3)^{1/2}$. By comparison, the temperature dependence of the resistance of an intrinsic or lightly doped semiconductor arises from the creation of mobile carriers by thermal excitation across a gap, so has the form $R=R_0\exp(\Delta/T)$, with $\alpha=-\Delta/T^2$. Because $\Delta\gtrsim 100$ K in available materials this phenomenon does not make thermometers for low temperatures with useful impedances. Ideally, the parameter chosen to express the temperature dependence of R should be itself independent of T. Mather[25] makes use of the parameter $TR^{-1}(dR/dT)$ to characterize thermometers. It has a weaker temperature dependence than does α for both of the exponential $R(T)$ functions described here and no temperature dependence at all for a power law dependence $R(T)=R_0T^n$.

Melt-doped semiconductors can be used as thermometers, but variations in N_A and N_D occur due to convection in the melt and segregation of impurities during growth that cause large variations in low temperature resistance. More uniform material is obtained by neutron transmutation doping (NTD) of ultrapure Ge, as described by Haller *et al.*[14,15] The nuclear reactions that occur in the stable isotopes of Ge yield Ga, As, and Se. A wide range of materials have been produced by this technique for use from 4.2 to below 20 mK. Data are shown in Fig. 6 for 25 samples of NTD-Ge which is adapted from Beeman and Haller.[37] The linear relationship between log resistivity and $T^{-1/2}$ indicates excellent agreement with theory.

One disadvantage of the NTD material has been that the compensation ratio is fixed by isotopic abundancies and nuclear cross sections to $N_D/N_A=0.32$, so that independent changes of R_0 and A can only be obtained by changes in thermometer dimensions. More freedom can be obtained by the use of isotope enriched Ge as was done by Itoh *et al.*[38]

Electrical contacts to Ge bolometers were long made with In solder, but with variable results. Nonthermal nonlinearities due to Schottky barriers and current dependent $1/f$ noise were often seen. These problems have been largely eliminated by the use of ion implantation followed by a thermal annealing cycle. A dose of 10^{14}–10^{15} 25–100 keV B ions/cm^2 for p-type Ge or Si or the same dose of P for n-type Ge or Si produces a degenerately doped p or n layer. The surfaces are then metallized with a ~20-nm-thick layer of Cr or Ti for adhesion followed by ~150 nm of Au for easy attachment to electrical leads.[14]

Large numbers of small (~200 μm^3) thermometers are now routinely produced from NTD-Ge. The boules are sliced into wafers which are etched to remove saw damage, ion implanted on both sides, annealed, metallized with Cr or Ti-Au, diced, etched, and passivated. Leads can be soldered with In, but are more often attached with small ~40-μm-diam dots of silver-filled epoxy. Wire bonding, which minimizes the effects of differential thermal contraction, is also useful.

Successful thermometers have also been made from melt-doped and ion implanted Si with ion implanted contacts by Moseley.[16] Because of the strong oxide on Si, soldered contacts are not successful. The compensation ratio can be varied, but the material is not as reproducible as NTD-Ge.

The resistance of Ge and Si thermometers depends on bias voltage, even when the lattice temperature is fixed, as described by McCammon *et al.*,[22] Kenny *et al.*,[39] and Grannan *et al.*[40] This effect arises from electric field dependent hopping at ^{4}LHe temperatures and hot electron effects at lower temperatures. It can be detected from its fast contribution to bolometer responsivity which invalidates some procedures for electrical measurements of responsivity.[24] These problems appear to be most serious for high background bolometers and x-ray bolometers which use relatively high bias.

B. Ge and Si chip bolometers

Ever since the pioneering work by Low,[8] small infrared bolometers $\lesssim(1\ \text{mm})^3$ have been produced from the Ge and Si thermometers described in the previous section. The bolometer size is selected to be comparable to the focal spot of the infrared. The thermometer material has strong bulk absorptivity due to photon assisted hopping between Stark-shifted impurity sites. There is, however, a significant surface reflectivity $R=(n-1)^2/(n+1)^2$ of nearly 36% in Ge which has index of refraction $n=4$ and 30% for Si with $n=3.4$. Antireflection coating is possible, but has been little used. Black paints have been used, but usually contribute excessive heat capacity. The semiconductor chip is usually supported on fine wire leads which also provide electrical contact and thermal conductance. Alloys such as brass are used for low background bolometers to obtain small values of G. Current technology for linear arrays of chip bolometers includes the use of 75-μm-diam 20 μm wall polyamide tubes for mechanical support. Metallized strips along the tubes provide electrical contact.[41]

When Si chip bolometers first became available, they developed the reputation of being better than Ge chip bolometers, largely because they were being compared with old style Ge chip bolometers, whose soldered contacts introduced excess noise and electrical nonlinearities. When implanted contacts are used for both Ge and Si chip bolometers, the differences arise from differences in heat capacity. The lattice specific heat per unit volume of Si is a factor ~ 5 smaller than for Ge. The Si chip bolometer can have advantages at ^{4}He temperatures where C often influences the bolometer NEP. At ^{3}He temperatures, however, this advantage is often not so important. The lattice heat capacity of both Si and Ge can then be negligible compared with contributions from metallic elements or epoxy. At even lower temperatures, the impurity heat capacity of the Si or Ge is expected to be larger than that of the lattice. Since a higher doping level is required in Si ($\sim 10^{-18}$ cm^{-3}) compared with Ge($\sim 10^{-16}$ cm^{-3}) Ge may have some advantages over Si below ^{3}He temperatures, if the other contributions to C can be made very small.

C. Composite bolometers

The chip bolometers described above combine the functions of radiation absorption and thermometry. There is a special problem for chip bolometers designed for high throughput millimeter wave systems. The bulk absorption coefficient of Ge and Si thermometer material with a useful resistivity decreases at low frequencies $\nu \lesssim kT_S/h$, since $h\nu$ becomes small compared with characteristic Stark shifts of majority carrier impurity energies that give significant phonon-assisted hopping at the sink temperature T_S. Consequently, bolometers for millimeter wavelengths must not only have large area $\approx A\Omega$, but must typically be one or more millimeters thick. The resulting heat capacity is a significant limitation. It was recognized quite early that improved performance could be obtained if these functions were separated. The author had limited success in 1961 with a sandwich bolometer for millimeter waves which used carbon resistor material as an absorber glued to a doped Ge thermometer.

In the context of a superconducting bolometer, the author[10] suggested a metallic film as the absorbing structure for composite bolometers for use at far infrared and millimeter wavelengths. This idea was quickly adapted by Werner *et al.*[42] for use with Ge chip thermometers. The absorber is a thin metal film with a sheet resistance of $\sim 200\ \Omega$ per square deposited on a thin transparent crystalline dielectric substrate with large thermal conductivity and high Debye temperature. This structure combines useful absorptivity with very small heat capacity per unit area. Early composite bolometers used sapphire substrates which have index of refraction $n\approx 3.2$ and have negligible absorptivity up to ~ 300 cm^{-1} at low temperatures. Diamond substrates with $n=2.5$ are transparent well beyond 1000 cm^{-1}. They are now widely used for low background bolometers at $T_S\sim 1$ K because of their small lattice specific heat. Silicon substrates with $n=3.4$ have larger lattice specific heat, but are useful for $T_S \ll 1$ K because the lattice heat capacity is small enough and they have smaller impurity heat capacity than diamond. Also, they can be produced by Si micromachining techniques as described below.

In order to obtain a frequency independent absorptivity, the metal film is placed on the back surface of the dielectric (away from the incident radiation) and the sheet resistance is selected[11] to be $R_\square = 377/(n-1)[\Omega]$. Since the impedance inside the dielectric is then matched to the parallel combination of the film and of free space, this is the condition for radiation inside the dielectric to exit through the metallized surface with no reflection. With no reflection at one surface there are no interference fringes and the absorptivity for normal incidence, $A=4(n-1)(n+1)^{-2}$, is independent of frequency. For sapphire, which is birefringent with an average $n\approx 3.2$, $R_\square = 200\ \Omega$ and $A=50\%$. The absorptivity is somewhat smaller for larger or smaller values of n. Clarke *et al.*[11] calculated the maximum and minimum values of the transmittance, reflectance, and absorptance as a function of $377/R_\square$ and compared the results with transmittance measurements of Bi on sapphire as is shown in Fig. 7. The interference fringes are observed to disappear at $377/R_\square \approx 2.2$ as expected. Nishioka *et al.*[43] showed that the calculated average of the absorptances for the TE and TM polarizations remains close to 50% out to angles of incidence approaching 90° as is shown in Fig. 8. Consequently, tightly focused beams can be used to minimize bolometer area. Larger values of absorptivity can be obtained[11,44] over a limited frequency range by making use of the interference fringes produced when $R_\square < 200\Omega$. For example, for sapphire with thickness $d=3\times 10^{-3}$ cm, the fringe separation $(2nd)^{-1}=52$ cm^{-1}.

The requirements for the metal absorbing film are that it have the required infrared sheet resistance and that its conductivity be large enough that its thickness can be neglected. For the sheet impedance to be real, interband transitions should not be important and the scattering rate must be faster than the infrared frequency. The absorber must also be stable, reproducible, and have low heat capacity. The semi-

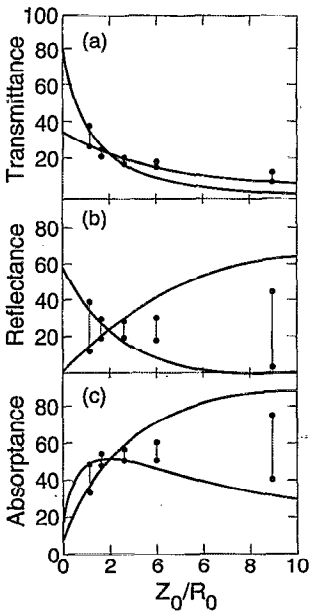

FIG. 7. Calculated maximum and minimum values of the Fabry–Perot fringes in the transmittance (a), reflectance (b), and absorptance (c) plotted as lines compared with values deduced from the measured transmittance of a Bi film on the back of a sapphire substrate plotted as dots. As expected, the fringes disappear for $377/R_\square = n - 1 = 2.2$ for sapphire.

metal Bi was chosen for its low conductivity. Evaporated Bi films with sheet resistances of 200 Ω are thick enough (≈60 nm) to be uniform, and the sheet resistance at submillimeter wavelengths is equal to the dc resistance. Because of the effects of impurities and boundaries this dc resistance must be measured on the thin film at low temperature.[11] The thickness of Bi required to obtain the desired $R_\square$ is minimized by allowing the substrates to get warm during evaporation or by annealing them after deposition. If the deposition scheme is reproducible, then a check of the dc resistance at low temperatures will ensure good absorber performance. The use of Bi at very low temperatures has been criticized by Dragovan and Moseley[45] because of the nuclear quadrupole contribution to the heat capacity. In the 60 nm thickness actually used, however, this effect is only important below 0.1 K.

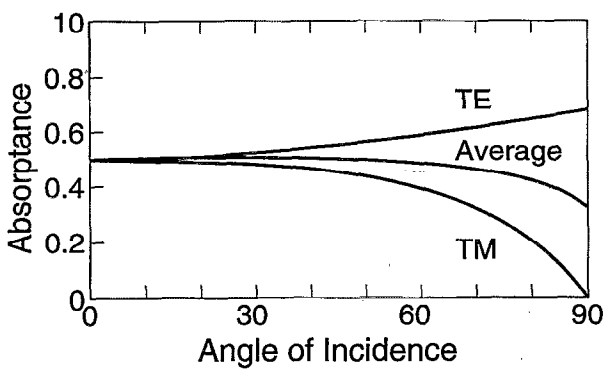

FIG. 8. Calculated absorptance as a function of angle for two polarizations for a 30-μm-thick sapphire substrate backed with a metal film with sheet resistance 188 Ω/□. These quantities have a weak frequency dependence. They have been averaged over the spectral range from 1 to 100 cm^{-1}.

In low temperature low background bolometers even the very small heat capacity of the absorbing film can be important. Since the conductivity is proportional to the product of the electron density times the conductivity relaxation time, while the electronic specific heat is proportional to the electron density, there is an advantage to a long relaxation time. The impurity and boundary scattering processes that limit the relaxation time in thin films of high conductivity metals are less effective in semimetals such as Bi because the low electron density gives long electron wavelengths. For this reason, the conductivity of very thin Bi films remains temperature dependent down to quite low temperatures. The lattice specific heat of Bi, however, is larger than the electronic contribution above ~0.3 K, as is shown in the Appendix.

Films of high conductivity metals can absorb radiation effectively but they must be very thin. Such thin films often have a nonuniform island structure. When this occurs, the infrared properties can be sensitive to the film morphology and cannot be reliably calculated from the low temperature dc resistance. Such thin films can oxidize completely, so they must either be resistant to oxidation (such as Au) or have a protective oxide (such as Al). Golay[46] used a granular Al absorbing film in his pneumatic detector.

It has been suggested that low heat capacity absorbers can be made using a superconducting metal with transition temperature T_c at a temperature $T \ll T_c$, where the electronic heat capacity is very small. The absorptivity in a superconductor is essentially that of the normal metal for frequencies above the gap frequency $\nu_g \approx 3.5kT_c$. However, Moseley[16] has expressed concerns about the possibility of noise arising from magnetic flux trapped in superconducting films.

Composite bolometers with Bi film absorbers on sapphire substrates are not generally used for frequencies above ~300 cm^{-1} because of the onset of lattice absorption in the substrate and interband transactions in the Bi. Diamond substrates with Au absorbers can be used past 600 cm^{-1}. In cases where large bolometer areas are required at higher frequencies gold black, which is described by Harris,[47] and Hoffman and Strond,[48] is a useful absorber. The absorptivity of gold black can be $\eta \sim 0.5$ at 300 cm^{-1} and it increases with frequency.

D. Examples of composite bolometers

Descriptions are given in this section of composite bolometers for millimeter and submillimeter wavelengths which are typical of current practice at several operating temperatures. The examples chosen are designed for use in low (negligible) infrared background since these bolometers provide some of the most severe challenges to the bolometer builder. Bolometers for higher backgrounds require larger values of G and can often tolerate larger values of C.

A good description of the composite bolometers built for use in the Cosmic Background Explorer Satellite at $T_S \sim 1.2$ K is given by Serlemitsos.[49] These use Au absorbers, diamond substrates, and doped Si thermometers.

Figure 9 from the recent work of Alsop *et al.*[50] shows the main features of a low background composite millimeter wave bolometer designed for use at ^{3}He temperatures. The 2 mm^2 35-μm-thick diamond substrate is coated with a 60-nm-

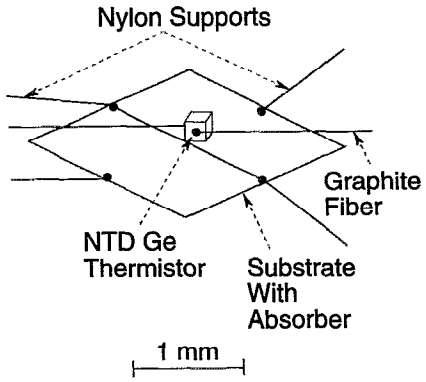

FIG. 9. Components of a typical low background composite bolometer.

thick Bi absorbing film on the backside and is supported on 15-μm-diam nylon fibers which are attached with dots of epoxy. These nylon fibers provide the dominant thermal conductance. The thermometer is a 200 μm cube of NTD-Ge that is attached to the diamond with epoxy. It has two ion-implanted and metallized faces; the electrical resistance is $R=3$ MΩ and temperature coefficient is $\alpha=21$ at 300 mK. Electrical contact to the thermistor without significant thermal conductance is obtained with 8-μm-diam graphite fibers which are attached with Ag-filled epoxy. The epoxy dots are typically 40 μm in diameter. The nylon and graphite fibers are supported from a metal ring with electrical contact pads. The mounting ring allows bolometers to be installed and interchanged without damage.

Although many composite bolometers resemble the one in Fig. 9 in most respects, a variety of materials options have been used. Sapphire substrates are often used in place of diamond in applications where the extra heat capacity can be tolerated. Metallic leads of brass or even copper are used to obtain larger values of thermal conductance. Kevlar support fibers have been used, but are not as satisfactory as nylon because their thermal expansion coefficient is very small. The significant contraction of nylon on cooling makes it easy to obtain high mechanical resonant frequencies $\gtrsim$300 Hz. A major concern for designers of composite bolometers is the thermal boundary resistance described in the Appendix between insulators and between metals and insulators at low temperatures. Some experimental evaluations of this effect are described in Lange *et al.*[13] The boundary resistance between the thermometer and the substrate can be important. However, the resistance between the absorbing film and the substrate is not generally important because of the large area involved.

Table I shows the performance that has been obtained for low background composite bolometers. These results are from the work of Serlemitsos[49] at $T_S=1.6$ K, Lange *et al.*[51] at $T_S=0.97$, Alsop *et al.*[50] at 0.30, and Clapp *et al.*[52] at 0.10. The rapid dependence of NEP on sink temperature T_S is noteworthy. These sensitivities are obtained only by very careful attention to details of materials and fabrication which are described in the references.

The values of NEP shown in Table I are very far below the NEP$=3$–10×10^{-10} W Hz$^{-1/2}$ typically obtained with

TABLE I. Electrically measured performance of composite bolometers from the work of Serlemitsos (Ref. 49), Lange *et al.* (Ref. 51), Alsop *et al.* (Ref. 50), and Clapp *et al.* (Ref. 52).

T_S (K)	1.6	0.97	0.30	0.10
A (mm^2)	40	16	4	4
S_E (V W^{-1})	...	1.3×10^7	8.7×10^7	1×10^9
NEP$_E$ (W Hz$^{-1/2}$)	4.5×10^{-15}	1.6×10^{-15}	1×10^{-16}	2.5×10^{-17}
τ_E (ms)	40	20	11	10

room temperature thermal detectors. It must be emphasized, however, that such low NEPs are only useful in applications which have negligible background. The classic application is with cooled optics on a space platform looking at dark regions of the sky. Depending on the bandwidth and the system efficiency such detectors can be used with ambient temperature optics from balloon and even airborne platforms at millimeter wavelengths.

It is of special importance to limit the background radiation on large area composite bolometers. Cooled low pass filters are widely used, but bandpass filters are essential for the highest sensitivity. To emphasize this point, we compare in Fig. 1 the achieved performance of low background composite (and chip) bolometers with the photon noise from 300 K radiation in a diffraction limited throughput, a 10% bandwidth, and various values of the product of emissivity ϵ of the background source, and the efficiency τ of the optical system divided by the absorptivity η of the bolometer.

Composite bolometers are available commercially for use with laboratory Fourier transform spectrometers which operate at 4.2 K with a low pass filter near $\sim$400 cm^{-1}. The signal power from the blackbody source in this example is many orders of magnitude larger than astronomical backgrounds. The technical challenge in making such bolometers is to obtain a large enough G without excessive C. The internal time constants of thermal links can be problem. Large area thermal contacts are useful to avoid thermal boundary resistances.

The infrared absorptivity of solid samples can be measured directly, rather than being deduced from transmittance or reflectance experiments, by using the sample as the absorber in a composite bolometer. A recent example of this technique applied to measurements of the absorptivity of high-T_c superconductors is given by Miller *et al.*[53]

E. Monolithic Si bolometers

Downey *et al.*[12] introduced a bolometer concept in which a thin Si substrate supported by narrow Si legs is micromachined from a Si wafer using the techniques of optical lithography. A conventional Bi film absorber was used on the back of the substrate, but the thermometer was created directly in the Si substrate by implanting P and B ions to achieve a suitable donor density and compensation ratio. The temperature dependences of the resistance obtained were qualitatively similar to those shown in Fig. 6 for NTD-Ge, with the advantages that the compensation ratio can be varied independently. Also there should be no thermal boundary resistance between the bolometer and the substrate. Although

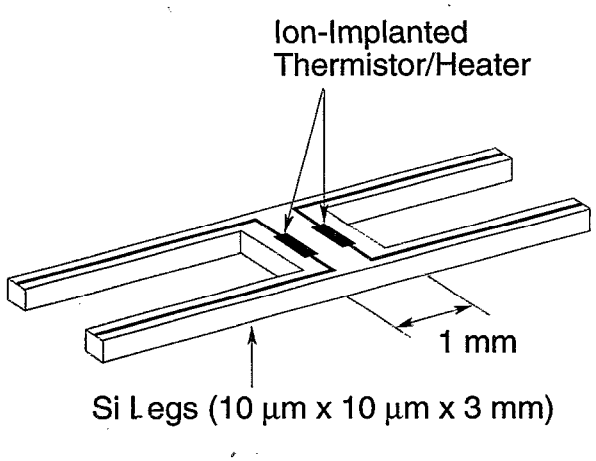

FIG. 10. Monolithic Si bolometer designed for x-ray applications.

the values of NEP_E reported for this early work are not as good as those for recent composite bolometers in Table I, it was shown clearly that ion implanted thermometers can have very small inherent $1/f$ noise and are well coupled thermally to the rest of the substrate. Once the required investment is made in technology, Si fabrication techniques can in principle produce excellent bolometers. In practice, much care is required to produce reproducible resistivities.

A new generation of monolithic Si bolometers has been developed for use as x-ray detectors by Moseley *et al.*[54] and McCammon *et al.*[22] These bolometers shown in Fig. 10 have small absorbing areas which could be made larger for infrared applications. They are equipped with two thermometers, one of which can be used as a heater for measurements of absorbed power responsivity. They have been produced in close-packed linear arrays.

A preliminary evaluation of this x-ray bolometer technology for very low background infrared space applications gave the lowest bolometer NEP known to the author. At $T_S=70$ mK, and negligible background, the measured responsivity was $S=3.5\times10^9$ V/W with $\tau_e=6$ ms. The amplifier noise limited absorbed power NEP measured by Timbie *et al.*[55] was 7×10^{-18} W Hz$^{-1/2}$.

One limitation of monolithic bolometers has been identified. The long wavelength phonons excited at low temperatures have long mean free paths in Si, so the legs of the bolometer act like phonon "light pipes." Even very long thin legs give larger G than is optimum for some applications. The long legs shown in Fig. 10 are not suitable for close-packed two-dimensional bolometer arrays.

One severe limitation of such low temperature low background bolometers is their saturation on relatively strong astronomical sources such as planets. This problem is less severe if the thermal conductance G increases rapidly with T. A 100 mK bolometer with $G=10^{-10}$ W/K which views Jupiter through a 1 m telescope will heat above 1 K if $G\propto T$ as is typical for metals but only to 400 mK if $G\propto T^3$, as is typical for insulators such as Si. Using the even stronger temperature dependence of G available from superconductors, it might be possible to design a bolometer which would remain BLIP limited over a very wide range of source power, despite saturation in the responsivity.

TABLE II. Contributions to the heat capacity of a composite bolometer from Alsop *et al.*

Material	C electron (J/cc K^2)	C lattice (J/cc K^4)	Volume (cc)	C at 330 mK (J/K)
Ag	6.3×10^{-5}	1.7×10^{-5}	6.7×10^{-9}	1.4×10^{-13}
Au	6.8×10^{-5}	4.5×10^{-5}	3.2×10^{-8}	7.7×10^{-13}
Pd	1.1×10^{-3}	1.1×10^{-5}	1.6×10^{-9}	5.6×10^{-13}
Ge	2.0×10^{-9}	3.0×10^{-6}	8.0×10^{-6}	8.7×10^{-13}
Graphite	6.1×10^{-6}	1.9×10^{-5}	2.0×10^{-7}	5.4×10^{-13}
Diamond	...	5.1×10^{-8}	1.4×10^{-4}	2.6×10^{-13}
Bi	3.8×10^{-7}	5.3×10^{-5}	2.4×10^{-7}	4.9×10^{-13}
Nylon	...	2.6×10^{-5}	1.6×10^{-6}	1.5×10^{-12}
Brass	9.7×10^{-5}	7.9×10^{-6}	2.0×10^{-7}	6.8×10^{-12}

F. Coupling of infrared and millimeter waves to bolometers

Since the heat capacity of most bolometers scales with area, bolometers are usually illuminated with a large solid angle to minimize the area for a given throughput. This is not an absolute requirement. The data in Table II suggest, for example, that in the absence of excess heat capacity only one-third of the heat capacity of this particular ^{3}He temperature composite bolometer would scale with the bolometer area. The Winston[56] light concentrator is often used to maximize the solid angle, especially for multimode throughput. In two dimensions, this device is an ideal concentrator. The three-dimensional concentrator is not ideal, but to a good approximation it rejects background power which arrives at the input at angles beyond cutoff and efficiently concentrates the power arriving at smaller angles into the maximum possible output solid angle. Since the exit aperture obeys Lambert's law, this maximum is $\Omega=\pi$. When the signal throughput approaches λ^2, the effects of diffraction cannot be neglected. A useful discussion of this topic in the astronomical context is given by Hildebrand.[57] The Winston cone has an approximately Gaussian antenna pattern when the throughput is limited to a single mode, $A\Omega\sim\lambda^2$. For this case, however, there seems to be little advantage over a simple straight cone antenna with a circular waveguide whose properties in the fundamental mode are well investigated by Murphy and Padman.[58] The straight cone is less favorable for multimode applications, however, since the angular cutoff of the incident beam is much less sharp as shown by Williamson.[59] Experiments by Fischer *et al.*[60] show that the accepted solid angle is not a sensitive function of the number of modes.

Winston cones are sometimes used with light pipe optics at both millimeter and submillimeter wavelengths. Figure 11 from Nishioka *et al.*[43] shows such a system used for measurements of the cosmic background radiation, which has features similar to many laboratory and astronomical systems. Winston cone *a* is used to define the throughput and reject background. Cone *b* partially recollimates the radiation so as to increase the efficiency of light pipes, filters, etc. Cone *c* condenses the radiation onto a composite bolometer which is located in a cavity to enhance its absorptivity. (In this particular case, the concentration for cone *c* was less

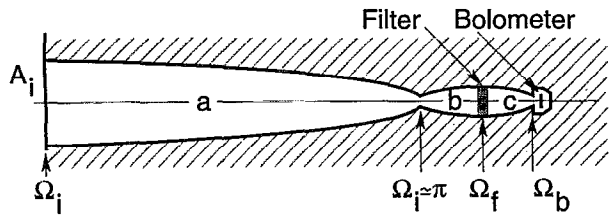

FIG. 11. Bolometer feed optics to limit background radiation. The Winston concentrator a defines the throughput $A_i\Omega_i$. The Winston concentrator b recollimates the radiation for a filter (as shown) or a spectrometer. The Winston $\Omega_f - \Omega_b$ converter reconcentrates the signal onto the bolometer which is located in a cavity.

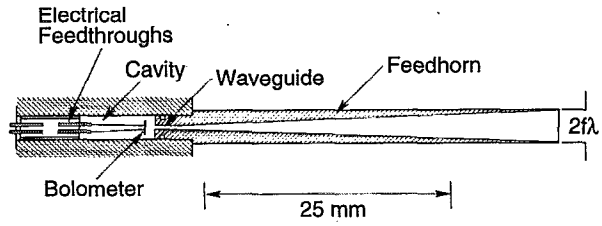

FIG. 12. The straight cone, circular waveguide, and cavity proposed for the 438 μm SCUBA diffraction limited array.

than for cone a, so that the system throughput is limited by only one aperture. Since many useful filters scatter or diffract radiation, using back-to-back Winston cones to define the throughput before filtering improves the antenna pattern of cone a. When diffraction is important, Mather[61] has used a flared apodizing horn. Single mode systems designed for use on astronomical telescopes often make use of reimaging mirrors rather than light pipes as described by Hildebrand[57] and by Cunningham and Gear.[62]

Since the absorptivities of most bolometers are less than unity, it is conventional to use a cavity to enhance the absorption. Much effort has been expended in the design of such cavities without really definitive results. A typical cavity contains an array of heavily damped standing waves, which is too complicated to analyze in detail. Some insight can be obtained from the random photon model due to Lamb.[63] This model,which was developed for irregular cavities with dimensions large compared to a wavelength, assumes that a photon in the cavity can be lost in several ways. If the photon distribution is sufficiently random, the probability of each loss mechanism is proportional to an effective black area, which is a physical area times an absorptivity. It suggests that the effective black area of the bolometer, which produces the signal, should be larger than the area of all of the holes plus the effective black area of the cavity walls. From this viewpoint, the use of a light concentrator is important because it minimizes the area of the coupling hole.

Ray tracing gives a precise analysis of cavity designs which, however, is not accurate because of diffraction. Hildebrand[57] suggests that the solid angle over which the bolometer sees itself reflected in the cavity walls should be minimized so as to maximize the solid angle over which it sees the source. If the cavity is fed by a partially collimated beam, then the detector should be tilted so that the reflected beam is trapped in the cavity. This is not so important for the large solid angle from a Winston cone. Despite the fact that quantitative optimization has not been done, the performance of sensible cavity designs is probably quite good, giving values of η from 70% to 90%.

When arrays of bolometers are used, aberrations limit the useful solid angle at the primary focal plane. Secondary lenses or Winston cones are still used to minimize bolometer area and to provide space between bolometers for mechanical support and thermal contact. Close packed arrays of NTD-Ge composite bolometers with T_S=0.1 K are being built for the JCMT telescope on Mauna Kea.[62] There are 91 bolometers for 438 μm and 37 bolometers for 855 μm. The feed optics shown in Fig. 12 includes a straight cone feeding a circular waveguide which is used in the fundamental mode. The severe constraints on space in a close-packed array and the need for long brass wires for the required G make the cavity space behind the bolometer larger than is desirable for maximum optical efficiency.

When composite bolometers are used to detect a relatively narrow band of wavelengths, then metal films can be used that produce interference fringes with peak absorptivities that approach unity.[11,44] At millimeter wavelengths, the required substrate thickness is larger than optimum, but the absorptivity can be high enough that no cavity is required and a relatively small area detector can be placed directly across the exit to the optical feed as done by Kreysa.[64]

In cases where single mode throughput is desired, it is possible to design a cavity which is simple enough in its fundamental mode to calculate and optimize its performance. Peterson and Goldman[65] have reported a design which achieves efficient coupling between a composite bolometer and a rectangular waveguide over the whole waveguide band. Such a system can have very good performance at near-millimeter wavelengths where very efficient waveguide filters and scalar horn antennas are available.

The approach used by Peterson and Goldman[65] for coupling of a single mode to a waveguide bolometer gives efficient coupling, but uses a Bi film-coated substrate whose thermally active volume is $>10^7$ μm^3. If the bolometer is used as the resistive load for an antenna, there is no fundamental limit to the area. As with a mixer diode, the active bolometer volume could be 1 μm^3 or even less. Ways in which this has been achieved are described below in the section on superconducting bolometers.

G. Electronics for semiconductor bolometers

The first stage of amplification for a bolometer output signal should not contribute significantly to the bolometer NEP. This condition can be met down to $T_S \sim 0.1$ K by JFET amplifiers at ambient temperature. For example, selected Toshiba 2SK147's have $V_A = 1\times10^{-9}$ V Hz$^{-1/2}$ and $I_A = 8\times10^{-16}$ A Hz$^{-1/2}$, giving T_N=0.03 K for the optimum bolometer resistance R=1.2 MΩ. However, the wires that connect high impedance bolometers to amplifiers are sources of microphonic noise. If a wire moves, its capacitance to ground changes. A voltage biased time varying capacitor gives a current $V_B dC/dt$ at the microphonic frequency. Ra-

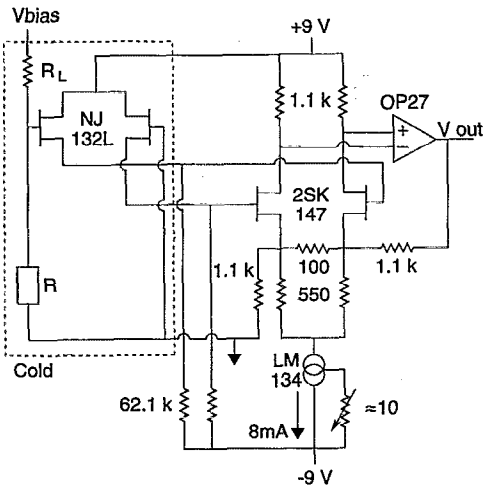

FIG. 13. Preamplifier used for ^{3}He temperature bolometer. The bolmeter is indicated by a rectangle and the cold portion of the circuit by a dashed line.

dio frequency pickup can also appear as a current source. Both sources of noise current create noise voltages $I_N R$ across the bolometer. The direct effect of these noise sources can be avoided if the microphonic and pickup frequencies are far from $\omega_S/2\pi$. However, the power $I_N^2 R_S$ is rectified by the bolometer, so time variations in $I_N^2 R_S$ can be a serious source of low frequency noise. Experience has shown that these problems can be minimized if the first stage amplifier is located inside the cryostat and rf filters are used on all leads entering the cryostat. The usual practice is to mount the amplifier on the LHe temperature cold stage and to heat it to the optimum operating temperature. When operated at 140 K, selected Interfet NJ132's have $V_A = 3\times10^{-9}$ V Hz$^{-1/2}$ and very low current noise at a few Hz. To obtain $T_N = 0.03$ K, R must be >5 MΩ. A pair of NJ132's will dissipate ~3 mW into the LHe. For applications where there is a severe rf environment, it is useful to enclose the bolometers and the first amplifier stage in a LHe temperature shield with LHe temperature rf filters. The signal can be introduced through a hole or a light pipe which acts as waveguide beyond cutoff for important rf frequencies.

An example of an amplifier circuit is shown in Fig. 13 from Alsop *et al.*[50] Matched JFET pairs are used to cancel common mode drifts. The load resistor is a series array of commercial 10 MΩ nichrome chip resistors with total $R_L \gg R$.

An extension of this drift cancellation idea, which can be important for astronomical applications, was investigated by Rieke *et al.*[66] Instead of grounding the gate of the second JFET, it was attached to a second load resistor and bolometer. In this way infrared signals common to both bolometers and the effects of drifts in T_S can be cancelled. The steady V_{bias} was replaced by an oscillatory bias at ~100 Hz and a lock-in amplifier so as to avoid $1/f$ noise in the amplifier. When components were carefully balanced it proved possible to avoid $1/f$ noise down to 0.05 Hz, so very slow sensitive bolometers can be used. This scheme with one bolometer illuminated and the other dark has been developed for the Infrared Telescope in Space (IRTS). This telescope has no chopper and is operated in the scanning mode so the infrared signals are modulated only very slowly as described by Devlin *et al.*[67] It is also being used by Glezer *et al.*[68] with both bolometers viewing the sky through a large ground-based telescope to cancel sky noise that is strongly correlated in the two beams.

H. Superconducting bolometers

Phase transition in solids can produce very sensitive thermometers over a restricted temperature range. For a useful thermal detector it is important to use a second order phase transition. Any latent heat would correspond to infinite heat capacity. The temperature dependence of the resistance of a metal film at the transition to superconductivity has long been considered for this application. Such thermometers can have low noise and are easily fabricated by thin film deposition and optical lithography so as to have very small volume. By controlling the metallurgy, a range of temperature coefficients from moderate to very high can be obtained. The parameter $\alpha = R^{-1} dR/dT$ is essentially the inverse of the width of the superconducting transition. Superconducting infrared bolometers have been discussed for many years, but have been hindered by the inherently low impedance of superconducting thermometers, which are therefore poorly matched to conventional amplifiers. There have been significant applications of superconducting bolometers to low temperature heat pulse and pulsed phonon experiments, which make use of the fast thermal time constant $\tau = C/G$, of a metal film with heat capacity C and a thermal boundary resistance G.

Current biased superconducting bolometers are subject to thermal runaway since with $\alpha > 0$ the power dissipated by a constant bias current increases with increasing temperature. From Eq. (6) runaway occurs when $G_e = G - J^2 R\alpha = 0$. This provides a limit to the useful bias current which is often set to $I \approx 0.3(G/R\alpha)^{-1/2}$. In principle, thermal runaway can be avoided by using a constant voltage bias and measuring the bolometer current.

Clarke *et al.*[11] carried out a detailed optimization of a superconducting transition edge bolometer for near-millimeter waves. An Al thin film thermometer operated at $T_c = 1.3$ K and a Bi film heater for calibration were evaporated on a sapphire substrate which was supported by nylon threads. Low impedance electrical contact to the thermometer and heater without excessive thermal conductance was obtained by evaporating superconducting In onto the nylon threads. The widely used Bi film radiation absorber described in 2.2 above was introduced in this work. The problem of low thermometer impedances $R \sim 3\Omega$ was solved by the use of an ac bolometer bias at 1 kHz, and a step-up transformer at low temperature which gave $T_N \sim 0.5$ K for the readout circuit. The bolometer was used in a bridge circuit to cancel the unmodulated alternating bolometer voltage which could otherwise cause excessive current in the transformer. The amplifier output was demodulated with a lock-in amplifier and fed back at low frequencies $\ll \omega_S/2\pi$ to a heater on the bolometer mount to keep T_S locked to the center of the superconducting transition.

This bolometer had an energy fluctuation noise limited absorbed power NEP$=1.7\times10^{-15}$ W Hz$^{-1/2}$ with an area of 16 mm^2 at $T_S=1.3$ K, which is excellent even by today's standards. It represented several important improvements in bolometer technology. Compared with contemporary Ge thermometers, the Al thermometers had little inherent $1/f$ noise and low heat capacity. The thermal feedback system reduced $1/f$ noise from fluctuations in T_S. The Bi film absorber gave high optical efficiency with low heat capacity. Despite these advantages, this bolometer was never used. In a remarkably short time, composite bolometers with Bi film absorbers and improved Ge thermometers[42,43] gave nearly equivalent performance with a simpler electronic readout.

Clarke *et al.*[11] also explored the use of superconducting quantum interference device (SQUID) amplifiers to read out low impedance thermal detectors. In this case, the thermometer was the temperature dependent critical current in a superconductor-normal metal-superconductor (SNS) junction. Again, excellent performance was achieved, but with significant complexity.

McDonald[69] has proposed a novel thermal detector which uses a SQUID to read out the temperature dependence of the kinetic inductance of a superconducting thin film below T_c where its ac resistance is essentially zero. This kinetic inductance arises from the inertia of the superconducting electrons, and its temperature dependence comes from thermal excitation of normal carriers as T approaches T_c. Like the pyroelectric detector, this kinetic inductance detector avoids the Johnson noise, which is an inherent property of the resistance thermometer in all bolometers. The tradeoff is the complexity of a bridge readout and the SQUID.

Since the noise in SQUID amplifiers can be very low, there are benefits to be obtained from the absence of Johnson noise. By reference to Eq. (23) we see that without Johnson noise or amplifier noise the NEP is independent of the responsivity S. This insensitivity of the detector NEP to S can be used to increase its dynamic range by using a thermometer with smaller α. The relatively modest values of α available from the kinetic inductance effect appear appropriate in this regard. Alternatively, the absence of Johnson noise allows the energy fluctuation noise to be reduced by reducing G. The resulting bolometer will be slow. It will operate with $\omega_S C/G \gg 1$, which is unconventional, but satisfactory for many experiments.

I. SQUID amplifiers

Since SQUID amplifiers are appropriate for low impedance superconducting bolometers, it appears useful to describe them here. Although rf SQUIDS can be used for bolometer readout, the dc version has advantages of simplicity that make it more appropriate. The operation of this device is illustrated in Fig. 14 adapted from Clarke.[70] The dc SQUID is based on the properties of the resistively shunted Josephson junction. Such junctions can carry lossless supercurrent up to a critical value I_0, above which they enter a resistive state. The I-V curve of the junction has $V=0$ for junction currents less than I_0 and develops a finite voltage for junction current $>I_0$. It approaches the voltage IR across the resistor for large junction current.

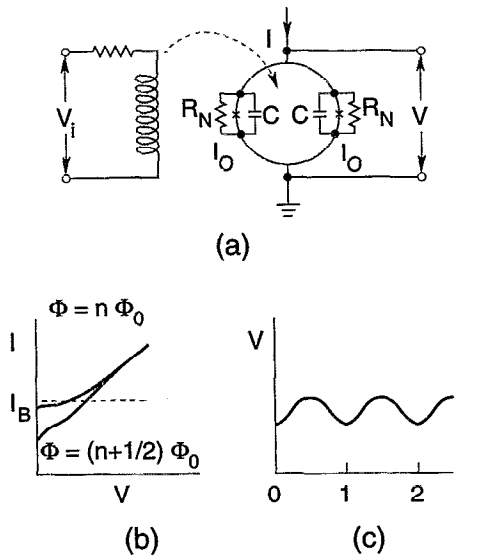

FIG. 14. (a) Equivalent circuit for a dc SQUID equipped with a coupling loop to convert a voltage V_i to an applied flux Φ. (b) SQUID I-V curves for applied flux Φ equal to n and $n+1/2$ times a flux quantum. (c) Voltage across current-biased SQUID as a function of applied flux.

The SQUID is the superconducting loop shown in Fig. 14(a) which contains two tunnel junctions that are shunted by resistors R_N and capacitors C. When an external current is driven across the SQUID loop as shown in (a) it divides between the two branches subject to the condition that the total magnetic flux Φ through the loop is quantized in units of the flux quantum $\Phi_0=h/2e=2.07\times10^{-15}$ Wb. When the externally applied flux Φ is equal to an integral multiple of Φ_0, this condition is satisfied with no circulating current. Then both junctions carry the same current and the critical current of the SQUID as a whole is $I=2I_0$. When the external flux does not equal $n\Phi_0$ then, to meet the quantization condition, there must be a circulating current, so one of the junctions will exceed its critical current for an overall SQUID current $I<2I_0$. The I-V curve of the SQUID is shown in Fig. 14(b) for the two cases $\Phi=n\Phi_0$ and $\Phi=(n+1/2)\Phi_0$. Also shown is the dashed load line for a constant current bias. As the external flux is increased, the SQUID voltage oscillates between the two I-V curves in Fig. 14(b) giving the response shown in Fig. 14(c). The SQUID is usually operated in a flux-locked mode with a feedback circuit to keep Φ constant. The output from the feedback loop current is able to resolve $\lesssim10^{-3}\Phi_0$. For use with bolometers, the SQUID can be operated as an ammeter or a voltmeter. The current to be measured passes through a multi turn coil that couples magnetic flux Φ into the SQUID as is shown in Fig. 14(a).

Modern dc SQUIDS are produced in robust Nb film technology by optical lithography. They occupy areas of $\sim1\times1$ mm, operate at any temperature below 4.2 K, dissipate $\sim10^{-9}$ W of power, and in bolometer circuits have noise temperatures below the ambient temperature.[70] Some of the current interest in developing low impedance superconducting bolometers arises from the advantages in power dissipa-

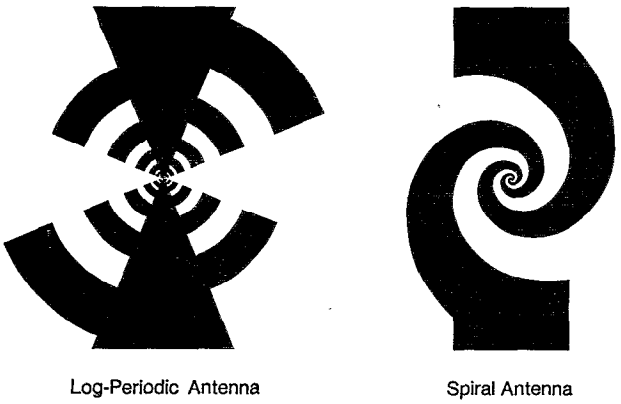

FIG. 15. Log periodic and spiral antennas. The microbolometer is located at the center.

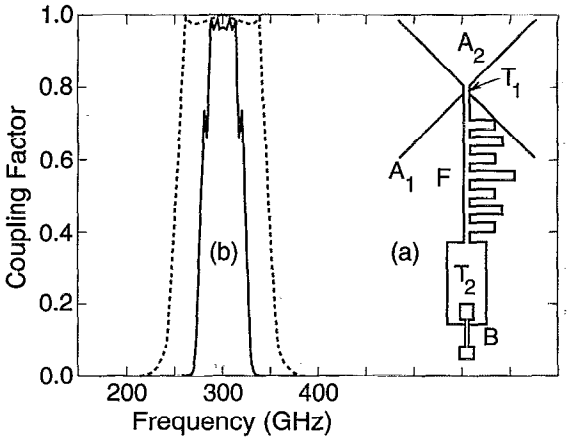

FIG. 16. (a) Example of a planar lithographed antenna with terminals A, and A_2 coupled to a microbolometer B by two microstrip impedance matching transformers T_1 and T_2 and a bandpass filter F. (b) Two calculated examples of the coupled bandpass.

tion and operating temperature of SQUID amplifiers over FET amplifiers.

J. Antenna-coupled microbolometers

Nahum and Richards[71] and Mees *et al.*[72] have described an antenna coupled superconducting microbolometer which has some attractive features for array applications. Based on the work of Hwang *et al.*[73] on room temperature Bi bolometers, this device uses a planar lithographed antenna to couple incident radiation into a thermally active volume with micron dimensions. The use of an antenna limits the throughput to one spatial mode with one polarization. This limitation to one mode is potentially useful for bolometers used for diffraction limited observations over a broad spectral range. Since the throughput varies as λ^2 for an antenna coupled bolometer, short wavelength background radiation is rejected more efficiently than by a conventional bolometer which has constant throughput over its useful range. The most useful antennas for this purpose are under development for use with superconducting heterodyne receivers. The include the log periodic and the log spiral shown in Fig. 15. Both have no characteristic length, so are inherently broad band. Both are self-complementary (the shape of metal is the same as the shape of the dielectric). Such antennas have a frequency independent real terminal impedance of $R=377(2+2\epsilon)^{-1/2}$ when deposited on a thick substrate with dielectric constant ϵ. For quartz with $\epsilon=4.4$, $R=115\ \Omega$. Antennas on thick substrates have the inconvenient property of radiating primarily into the substrate, which is usually shaped into a dielectric lens as described by Rutledge *et al.*[74] or mirror to obtain a useful free space antenna pattern. Recent experiments by Grossman *et al.*[75] suggest that free space radiation with wavelengths as short as 19 μm will couple efficiently into log spiral antennas. Other planar submillimeter wave antennas are under development. These include the twin slot antennas described by Henston *et al.*[76] and the slot line end fire antennas described by Ekström *et al.*[77]

In the antenna-coupled microbolometer, a thin narrow strip of superconductor is connected between the antenna terminals. When operated near T_c, this film acts both as a resistive load to convert the infrared current into heat and a thermometer to measure the temperature rise. The bolometer is deposited directly on a transparent dielectric substrate such as fused silica. Such bolometers are inherently very fast—often much faster than applications require. Useful values of NEP are obtained only when care is taken to minimize the thermal conductance G. The small size of the thermally active region is useful in this regard as it produces a thermal spreading resistance. The thermal boundary resistance described in the Appendix can also be important. If the thermometer film is thin enough, the transfer of heat from the electrons to the substrate can be limited by the electron phonon interaction inside the thermometer. Heat flow from the film into the antenna is greatly reduced if the antenna is made from a superconductor with energy gap larger than that of the thermometer. When this condition is met, thermally excited normal electrons (quasiparticles) in the thermometer are reflected at the antenna terminals and are trapped in the thermometer. Because of the small heat capacity such bolometers are very fast. The calculated $\tau \approx 10^{-8}(1\ \mathrm{K/T})^2$ s gives 10^{-8} s for a bolometer operating at $T=1$ K. Despite this speed the calculated absorbed power $\mathrm{NEP}_A=8.4\times10^{-16}$ (T/1 K)$^{5/2}$ W Hz$^{-1/2}$ gives 2.6×10^{-18} W Hz$^{-1/2}$ at $T=100$ mK.

Interest in this antenna coupled microbolometer is enhanced by the possibility that it could be produced by lithography in large format arrays with integrated SQUID readouts. Mees *et al.*[72] have considered the use of superconducting microstrip technology at millimeter wavelengths to couple the thermometer to the antenna. Such microstrips are well developed for use in Josephson effect digital circuits. Once this is done, impedance transformers can be used to match the film resistance to the antenna and filters can be introduced to control the bolometer bandpass. Figure 16 adapted from Mees *et al.* shows how such a coupling structure could be implemented. The antenna terminal A_1 forms the ground plane for the microstrip. This is covered with a SiO_x insulator. The second antenna terminal A_2 and the microstrip are deposited over the insulator. In the configuration shown, two impedance matching transformers T_1 and T_2 and also a seven-element Chebyshev filter F are located between

the 100 Ω antenna terminals and a 2 Ω thermometer. The coupling factor calculated for realistic film properties shows that values approaching unity can be obtained over a sharply defined bandpass. Without the coupling structure the coupling coefficient for such a large impedance mismatch would only be ~0.1.

A novel hot electron microbolometer with considerable promise for low background measurements at near-millimeter wavelengths has been suggested by Nahum, Mears, and Richards.[78] The antenna is terminated in a thin copper strip. The electron phonon interaction at low temperatures is weak enough that the infrared photons heat the copper electrons significantly. The electron temperature is measured by the tunneling current in a copper/aluminum oxide/aluminum tunnel junction. The effective thermal conductance G from the electron phonon interaction depends on the volume of copper. Very small values appropriate for low background measurements are easily obtained. Experiments by Nahum and Martinis[79] have verified the predicted device performance using a steady current as the signal source and obtained values of $NEP_E < 10^{-18}$ W Hz$^{-1/2}$ at 0.1 K. Since the tunnel junction readout depends exponentially on temperature and the effective thermal conductance G varies as T^4, this device has a much wider dynamic range than the transition edge microbolometer and saturates only gradually at high power.

The superconducting bolometer technologies described in this section are generally not mature. They have not been used in significant applications. Many possibilities exist that have not been attempted, or even thoroughly analyzed. For example, the microbolometer can be waveguide coupled at millimeter and even submillimeter frequencies using techniques developed for diode mixers. The dynamic range limitations of transition edge bolometers can be overcome by the use of feedback at ω_S as is done for the SQUID. The thermometer and the self-complementary antenna can be deposited on a thin membrane to obtain lower values of G and thus lower NEP as well as possibly increased optical efficiency. The possibilities are endless, but it should be kept in mind that the criterion for real success is a device that does an important job better than the competition.

K. Composite high-T_c bolometers

Bolometers that use the resistive transition near 90 K in a high-T_c superconductor as the thermometer are of interest since there are many applications for infrared detectors in which LN is acceptable as a coolant and LHe is not. As described in Sec. I A, there is no satisfactory LN temperature detector technology for infrared wavelengths much beyond 10 μm. Consequently, room temperature thermal detectors are widely used in applications where an optimized LN temperature thermal detector could give much better performance. Of course, any LN-cooled thermal detector will be orders of magnitude less sensitive than a LHe-cooled bolometer.

Many groups independently recognized that the discovery of superconductivity in $YBa_2Cu_3O_7$ with $T_c = 90$ K provided a suitable thermometer for a LN-cooled bolometer.

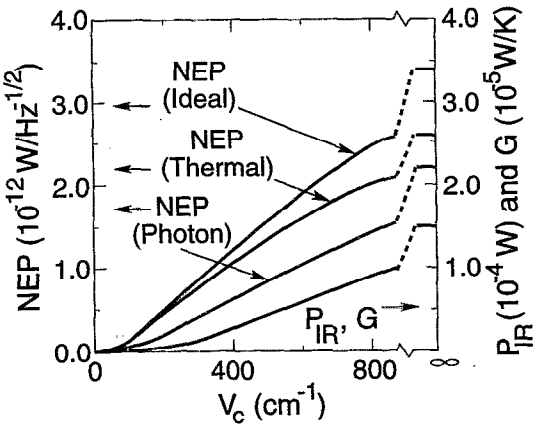

FIG. 17. Infrared power loading P_{IR} and thermal conductance G for an ideal thermal infrared detector plotted as a function of the cutoff frequency ν_c of the cold low pass filter. The detector is assumed to view 300 K background radiation with a throughput $A\Omega = 10^{-2}$ sr cm^2 and perfect optical efficiency and to operate 10 K above the heat sink temperature of 80 K. The NEP of the ideal detector is shown along with the separate contributions from thermal (energy fluctuation) noise and photon noise.

The performance of the first primitive devices, however was often orders of magnitude worse than that of the room temperature pyroelectric detector.

The performance of an ideal bolometer limited only by photon and phonon noise and operated at 90 K with $T_S = 80$ K was calculated by Richards *et al.*[80] They assumed a cooled low pass filter and other parameters appropriate for a detector designed to extend the long wavelength range of a chemical laboratory Fourier transform infrared spectrometer. As shown in Fig. 17 from Richards *et al.*, the calculated NEP is more than 100 times better than the ~5×10^{-10} W Hz$^{-1/2}$ available from commercial pyroelectric detectors. This illustrates that LN-cooled bolometers are useful in principle.

The materials requirements for a competitive high-T_c bolometer, however, are quite severe. To achieve sufficient responsivity that Johnson noise and amplifier noise are small, it is necessary to have a narrow transition width $\approx\alpha^{-1}$. Also, current-biased YBCO films show $1/f$ voltage noise which arises from resistance fluctuations. Both the transition width and the noise are minimized in the very highest quality c-axis epitaxial films, which can only be produced on very specific crystalline substrates (or crystalline substrates coated with thin epitaxial buffer layers).

Except for diamond, most suitable substrate materials for composite bolometers have similar volume specific heat at 90 K. In all cases, it is very much larger than is seen at LH temperatures. Consequently, even when a value of G appropriate for 300 K backgrounds is selected, as in Fig. 17, the thermal time constant tends to be very long. Therefore, one important requirement for a substrate material is strength, so that it can be made very thin. Thin film high-T_c thermometers are favored to minimize heat capacity with a narrow strip configuration to maximize the electrical resistance. Some substrates that are favorable for film growth, such as $SrTiO_3$ and $LaAlO_3$ are too weak to produce thin layers of millimeter dimensions.

A high-T_c thermometer can be characterized by a noise equivalent temperature NET$=\Delta R/\alpha R$ (K Hz$^{-1/2}$). Verghese *et al.*[81] have measured values of 3×10^{-8} K Hz$^{-1/2}$ for YBCO on a $SrTiO_3$ buffer layer on sapphire, and 8×10^{-8} for YBCO on a YSZ buffer layer on Si. An otherwise very favorable polycrystalline substrate material Si_3N_4, with a YSZ buffer layer, gave a much less favorable 2.4×10^{-6}. For comparison, the NET is $\sim10^{-6}$ K Hz$^{-1/2}$ for a pyroelectric detector. Diamond has not been much used despite its favorable heat capacity partly because of the cost of the large number of crystalline substrates needed in the development process and partly because carbon degrades YBCO films. It may be possible to produce high quality films on diamond by the use of buffer layers.

Verghese *et al.*[81,82] have produced a 1×1 mm composite bolometer with Au black absorber on 20-μm-thick sapphire substrate which has $S=19$ V/W with a resistance $R=5$ Ω. The NEP was 2.4×10^{-11} W Hz$^{-1/2}$ at 10 Hz with $\tau=55$ ms. Assuming that the excess noise in a better sample would be less than Johnson noise, this NEP could be improved to 10^{-11} W Hz$^{-1/2}$ at 10 Hz which corresponds to $D^*=10^{10}$ cm Hz$^{1/2}$ W^{-1}. This detector was successfully used with a step-scanned infrared Fourier transform spectrometer and gave a significantly better signal-to-noise ratio than a good commercial pyroelectric detector. This group has also produced a 3×3 mm^2 detector with a Bi film absorber for use at near-millimeter wavelengths.

Brasunas *et al.*[83,84] have used a somewhat different approach to the substrate problem. They have lithographed a high resistance meander strip of YBCO on a small chip of $SrTiO_3$ and glued it to a larger area substrate coated with a metal film absorber. This composite approach makes it possible to use a material that is favorable for film deposition but with poor mechanical properties, together with a thin strong substrate, which could be diamond. The measured performance, however, has shown larger $1/f$ noise than is expected from high quality films. Although it is possible that the films were damaged in the lithography used to produce a high resistance meander line in a small area, it is also possible that the $1/f$ resistance fluctuations are enhanced in films of small volume.

The bolometer of Verghese *et al.*[81,82] is an existence proof for a competitive high-T_c bolometer, not an optimized device. It was produced by a low yield process involving thinning the sapphire after YBCO deposition. Lower heat capacity is needed to produce a detector fast enough for use with a rapid-scan Fourier transform spectrometer. Lower thermometer noise is required for an optimum NEP. Higher thermometer impedance is required so as to avoid the use of a transformer-coupled amplifier. Bipolar transistor amplifiers can have $T_N<100$ K for $R>200$ Ω.

It should be possible to obtain significantly improved performance in this type of high-T_c bolometer by the use of membrane substrates with thickness $\lesssim1$ μm. Stratton *et al.*[85] and Johnson[86] have described fabrication of YBCO high-T_c bolometers on polycrystalline Si_3N_4 membrane substrates with membrane support legs. The resulting bolometers give $D^*=7\times10^8$ at 7 Hz. Using values of the measured properties of YBCO films on buffer layers on Si and Si_3N_4 (on Si),

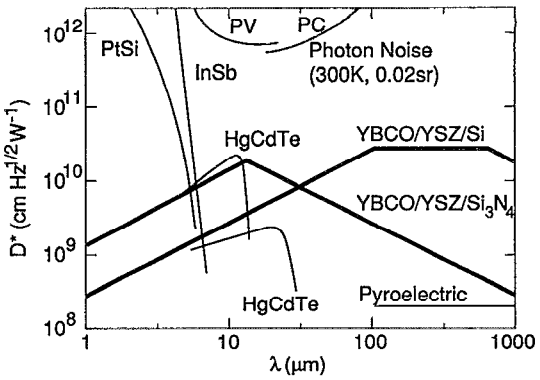

FIG. 18. Specific detectivity D^* as a function of wavelength for diffraction-limited pixels with $\Omega=0.02$ sr ($f/6$ optics) and $\tau=10$ ms. The thick lines show the predicted D^* for the high-T_c bolometers on silicon and Si_3N_4 membranes using YBCO thermometers. These lines were calculated using estimates for the minimum achievable heat capacity and thermal conductance and using measurements of voltage noise high-T_c thermometers. Typical values of D^* for InSb, PtSi, and HgCdTe detectors in two-dimensional staring arrays operated at 77 K are shown for comparison. Also shown are the photon noise limits for photovoltaic and photoconductive detectors which view 300 K radiation in a 0.02 sr field of view.

Verghese *et al.*[87] have calculated the performance of high-T_c membrane bolometers with $\tau\leqslant10^{-2}$ s, diffraction limited throughput and $f/6$ optics. These parameters are appropriate for diffraction limited infrared imaging. Their results are shown in Fig. 18 as a plot of the wavelength dependence of the specific detectivity D^*, which can be as high as 3×10^{10}. Also shown, for comparison, are the photon noise limited D^* and estimates of the performance of detectors now used in large format imaging arrays.

Ideally, D^* should be independent of bolometer area and thus of wavelength in Fig. 18. On these plots, however, D^* falls at short wavelengths because the membrane technology is not able to provide a small enough G for a small detector area, and τ becomes shorter than 10^{-2} s. It also falls at long wavelengths because the resistance fluctuation noise becomes important in large area detectors. The D^* of the Si_3N_4 membrane bolometer has a potentially useful peak near 10 μm, which is a very important wavelength for thermal imaging. The D^* of the Si membrane bolometer peaks at longer wavelengths because of the higher thermal conductivity of Si and the lower NET of YBCO films on Si. These calculations confirm that membrane bolometers will be very useful if they can be built without degrading the values of NET already achieved for YBCO films on supported membrane materials.

Nearly all work on high-T_c bolometers make use of films of $YBa_2Cu_3O_7$ with $T_c\sim90$ K which are well adapted to bolometers cooled with LN. In principle, other superconductors could be used, e.g., the BSCCO family with T_c near 90 K or the *Tl* based materials with T_c up to 125 K. In practice, very much less is known about substrates, film deposition conditions, noise, lithography, and all of the other technologies required for the use of these materials. If an application develops for a ~25 K bolometer, the BKBO family of superconductors might prove useful. They may be easier to work with than YBCO because of their cubic crystal structure.

L. High-T_c microbolometers

The antenna-coupled microbolometer concept described in Sec. II J above has been proposed by Hu *et al.*[88] as a high-T_c device and implemented by Nahum *et al.*[89] The thermometer load was a $0.1\times6\times13$ μm^3 strip of YBCO deposited directly on a low thermal conductivity substrate of YSZ (ZrO_2 stabilized with Y_2O_3). Thermal isolation was provided by the thermal spreading resistance into the substrate giving a fast response extending beyond 10^4 Hz. Electrical measurements of the responsivity and noise showed an energy fluctuation noise limited NEP$=4.5\times10^{-12}$ W Hz$^{-1/2}$ which is nearly a factor 10 lower than the high-T_c composite bolometer. The measured performance was in excellent agreement with theory. Although this high-T_c microbolometer is very promising, it has significant limitations. The low NEP is only obtained for modulation frequencies above 1 KHz where the $1/f$ noise is small. The YSZ substrate strongly absorbs submillimeter wavelengths. Better performance in most applications could be obtained if the bolometer were deposited on a thin membrane to decrease G and reduce the absorption in the substrate. In this case, no dielectric lens would be required.

M. Other high-T_c detectors

There has been much interest in the possibility of nonbolometric high-T_c detectors. Response of current-biased granular YBCO films to infrared and visible photons has been observed well below T_c that does not scale with dR/dT. It appears that this response is due to thermally activated magnetic flux motion that generates an emf across the film. Leaving aside the question of whether this effect should be included under the general definition of a bolometer given in this review, it is not likely to be useful because of the very large noise in current-biased granular films. Such films can be thought of as a multiply connected array of SQUIDS. Small disturbances trigger switching between many states with different current distributions causing large noise.

Many workers have measured the response of high quality epitaxial YBCO films on thick substrates to fast laser pulses. A substantial response with a time constant of a few ns is typically seen which is much faster than the thermal relaxation time for heat propagating through the substrate. The bolometric nature of this response was demonstrated by Nahum *et al.*[90] They measured a boundary resistance between YBCO and various substrates which was large enough to give a nanosecond thermal time constant for the film relative to the substrate. Carr *et al.*[91] reached the same conclusion based on comparisons between the responsivities and time constants for films with various thicknesses. This fast high-T_c bolometer is potentially useful with pulsed infrared sources such as synchrotron storage rings. Response due to changes in kinetic inductance has also been seen in high T_c films.

Like most materials, YBCO and other high-T_c superconductors show even faster response due to hot electrons which is probably essentially thermal. As with other thermal effects, a very fast observed response implies a small responsivity, unless very small numbers of electrons are involved.

N. Conclusions

Bolometric detectors for infrared and millimeter waves are a wide versatile class of devices which have a long history of active development and many successful applications. However, a number of apparently possible applications, such as large format arrays and ideal LN temperature operation have yet to be demonstrated. There is room for much improvement.

ACKNOWLEDGMENTS

The author is most grateful to the Experimental Cosmology Group of the Department of Physics at the University of Rome "La Sapienza" and to the Radio Astronomy Group of the Department of Physics at the Ecole Normale Superieure in Paris for their hospitality during the preparation of this review. Special thanks are due to S. Verghese for discussions about low frequency photon noise. This work was supported in part by the Director, Office of Energy Research, Office of Basic Energy Sciences, Materials Sciences Division of the U.S. Department of Energy under Contract No. DE-AC03-76SF00098.

APPENDIX: THERMAL PROPERTIES OF BOLOMETER MATERIALS

The successful design and construction of infrared bolometers requires detailed knowledge of the properties of materials at the appropriate temperatures. Simple theoretical models are used to guess what materials will be useful. Accurate experimental data are essential to produce optimized devices. Here we will summarize some of the most useful theoretical models and give references to collections of useful data. Workers not trained in solid state physics should start with a standard textbook such as Kittel.[92]

The heat capacity of any solid has a contribution from the thermal excitation of lattice vibrations (phonons) with $h\nu\approx kT$. The Debye theory gives the lattice specific heat in terms of a universal function of T/Θ which increases as T^3 for $T\ll\Theta$ and approaches a constant for $T>\Theta$. Most bolometers operate in the low temperature limit, so $C=234Nk(T/\Theta)^3$ [J/K] where N is the number of atoms. Values of Θ are large in light stiff materials such as diamond (2230 K), sapphire (1200 K), and Si(645 K) and are smaller in heavy or soft materials such as Ge(363 K), Cu(343 K), and Au(164 K). This range of Θ corresponds to an enormous range in lattice heat capacity at low temperatures.

For $T\ll\Theta$, where the bulk ideal lattice C is very small, many other effects can contribute significantly to the total heat capacity. The presence of weakly bound heavy impurities can increase the number of modes with $\hbar\omega\approx kT_S$. Excess heat capacities have been measured in composite bolometers at 0.3 K which may be due to impurities in sapphire[50] and diamond. Helium adsorbs on metals as a two-dimensional gas with a large heat capacity of ~1 Boltzmann constant per atom which can be seen for $T\lesssim1$ K as shown by Kenny and Richards.[93] This gas can be desorbed by heating the bolometer above ~5 K and adsorbing the gas on other cold surfaces. A wide variety of magnetic phenomena also contribute to the heat capacity and should be avoided.

The free electrons in a metal are a degenerate Fermi gas. They contribute a heat capacity $C_{el}=\gamma T$ where $\gamma=\pi^2k^2mN/\hbar^2(3\pi^2N/V)^{2/3}$, m is the effective mass, N is the number of electrons, and V is the volume. For the noble metals with one free electron per atom $\gamma\sim7\times10^{-4}$ J/mol K^2 and the electronic contribution typically becomes comparable to the lattice contribution at a few K. It is much smaller for semimetals such as Bi and for doped semiconductors because of the smaller effective mass and the smaller value for N/V. At finite temperatures, a superconductor can be thought of as consisting of superconducting electrons which are in a zero entropy state and contribute no heat capacity and thermally excited normal electrons with the Fermi gas heat capacity. The heat capacity of a superconductor increases exponentially with T for $T<T_c$ and then falls sharply at T_c to the normal state value $C=\gamma T$.

There is a very large literature describing experimental heat capacities extending over many years, most of which is oriented to special effects such as phase transitions, nuclear contributions, etc. Except for one extensive review of the specific heat of metals at low temperatures by Phillips,[94] the author is not aware of compilations that are really useful for builders of low temperature bolometers. Computerized literature searches, however, can be very successful. Handbooks are useful at 77 K. Primary references in the literature give specific heats per mol. Values normalized per unit volume are more useful for bolometer design.

Table II from Alsop *et al.*[50] gives the temperature dependent lattice and electronic contributions to the specific heat per unit volume expected for a number of bolometer materials. It is interesting to note that values for these quantities cited in different bolometer papers do not always agree. This data set is reproduced here because the authors give their primary references. Also shown in Table II are typical volumes of each material used in a composite bolometer and total contributions to the heat capacity at 330 mK. As mentioned above, however, the assembled bolometers showed significant excess heat capacity.

The thermal conductivity of a gas of free particles of density N/V and specific heat per unit volume c can be understood from kinetic theory to be $\kappa=cvl/3$, where v is the particle velocity and l is the mean free path. In an insulator, the particles are phonons, so $c\propto T^3$ from the Debye theory, v is the velocity of sound, and the mean free path l increases with decreasing temperature and then approaches a constant set by impurities and defects. Since v is not a sensitive function of T, there is a tendency for κ to vary as T^3 at low temperatures and then fall at higher temperatures where c approaches a constant and l decreases due to phonon–phonon scattering.

In metals, most of the heat is carried by the free electrons. Then $c_{el}\propto T$, $v=v_F$ is the Fermi velocity which is independent of T, and l is the electronic mean free path. Since l increases with decreasing temperature as electron phonon scattering is reduced and then saturates at the value set by impurities (or sometimes by the sample size), κ varies as T at low temperatures with a coefficient that depends on sample quality and falls with T at high temperatures in a more nearly universal way.

Since the electrical conductivity of a metal $\sigma=Ne^2l/mv_F$, the mean free path divides out of the ratio κ_{el}/σ. The result is the very useful Wiedeman–Franz law, $\kappa_{el}/\sigma=\mathscr{L}T$, where $\mathscr{L}=\pi^2k^2/3e^2=2.5\times10^{-8}$ WΩ/K^2. It is often convenient to obtain κ_{el} for a specific metallic sample from the handbook value of σ at 300 K which is insensitive to purity or size and a measurement of the ratio of σ at 300 K to that at the desired low temperature by a four-terminal technique. This resistivity ratio can be as small as 2 for an alloy or a thin film and as large as 10^5 for a pure single crystal. The Wiedeman–Franz law is well obeyed in all metals, except in the superconducting state. Superconducting electrons have infinite dc electrical conductivity, but cannot carry heat, so κ_{el} drops rapidly below T_c as the thermally excited (normal) carriers disappear. Very useful compilations of κ are given by Lounasmaa[95] for $T<1$ K and by the National Bureau of Standards[96] for $T>1$ K.

Significant thermal boundary resistances occur between a metal and an insulator or between two insulators because heat is carried across the boundary by phonons and because the acoustic impedances are different in different materials. When the effect of phonon reflection at the boundary is calculated, there is a thermal boundary resistance $R_{Bd}=\Delta TA/P=B/T^3$ which can be very important at low temperatures. Typical values of $B=20$ K^4 cm^2/W. Some specific values are given by Lounasmaa.[95] The boundary resistance between two metals depends on the reflection of electrons and is too small to be important.

Two idealized thermal geometries are very useful for bolometer design. The thermal time constant for an isothermal heat capacity C connected to a constant temperature heat sink by a thermal conductance G with no internal heat capacity is $\tau=C/G$. Alternatively, the internal relaxation time for one-dimensional heat flow over a length L through a medium with volume specific heat c and thermal conductivity κ is $\tau=cL^2/\kappa$. Using the simple model for κ described above, this can be written $\tau=3L^2/vl$. The internal thermal relaxation times for metals are much faster than for insulators because typical Fermi velocities are $>10^2$ times typical sound velocities.

[1] W. Herschel, Philos. Trans. R. Soc. **90**, 284 (1800).
[2] S. P. Langley, Nature **25**, 14 (1981).
[3] R. A. Smith, F. E. Jones, and B. Chasmar, *The Detection and Measurement of Infrared Radiation* (Clarendon, Oxford 1957).
[4] D. H. Andrews, W. F. Brucksch, W. T. Ziegler, and E. R. Blanchard, Rev. Sci. Instrum. **13**, 281 (1942).
[5] W. S. Boyle and K. F. Rogers, Jr., J. Opt. Soc. Am. **49**, 66 (1959).
[6] J. Cooper, Rev. Sci. Instrum. **33**, 92 (1962).
[7] A. Hadni, J. Phys. **24**, 694 (1963).
[8] F. J. Low, J. Opt. Soc. Am. **51**, 1300 (1961).
[9] N. Coron, G. Dambier, and J. Leblanc, in *Infrared Detector Techniques for Space Research*, edited by V. Manno and J. Ring (Reidel, Dordrecht, 1971), pp. 121–131.
[10] J. Clarke, G. I. Hoffer, and P. L. Richards, Rev. Phys. Appl. **9**, 69 (1974).
[11] J. Clarke, G. I. Hoffer, P. L. Richards, and N-H. Yeh, J. Appl. Phys. **48**, 4865 (1977).
[12] P. M. Downey, A. D. Jeffries, S. S. Meyer, R. Weiss, F. J. Bachner, J. P. Donnelly, W. T. Lindley, R. W. Mountain, and D. J. S. Silversmith, Appl. Opt. **23**, 910 (1984).
[13] A. E. Lange, E. Kreysa, S. E. McBride, P. L. Richards, and E. E. Haller, Int. J. Infrared Millimeter Waves **4**, 689 (1983).
[14] E. E. Haller, N. P. Palaio, M. Rodder, W. L. Hansen, and E. Kreysa, in *Proceedings of the Fourth International Conference on Neutron Transmu-*

tation Doping of Semiconductor Materials, edited by R. D. Larrabee (Plenum, New York 1984), pp. 21–36.
[15] E. E. Haller, Infrared Phys. **25**, 257 (1985).
[16] S. H. Moseley (private communication, 1990).
[17] H. D. Drew and A. J. Sievers, Appl. Opt. **8**, 2067 (1969).
[18] M. A. Kinch and B. V. Rollin, Br. J. Appl. Phys. **14**, 672 (1963).
[19] T. G. Phillips and K. B. Jefferts, Rev. Sci. Instrum. **44**, 1009 (1973).
[20] E. M. Gershenzon, G. N. Gol'tsman, Y. P. Gousev, A. I. Elant'ev, and A. D. Semenov, IEEE Trans. Magn. **MAG-27**, 1317 (1991).
[21] P. L. Richards and L. T. Greenberg, in *Infrared and Millimeter Waves* (Academic, New York 1982) Vol. 6, Appendix I.
[22] D. McCammon, M. Juda, J. Zhang, S. S. Holt, R. L. Kelley, S. H. Moseley, and A. E. Szymkowiak, Jpn. J. Appl. Phys. **26**, Suppl. 26-3 (1987).
[23] R. C. Jones, J. Opt. Soc. Am. **43**, 1 (1953).
[24] J. C. Mather, Appl. Opt.**23**, 3181 (1984).
[25] J. C. Mather, Appl. Opt. **23**, 584 (1984).
[26] M. J. Griffen and W. S. Holland, Int. J. Infrared Millimeter Waves **9**, 861 (1988).
[27] J. M. Lamarre, Appl. Opt. **25**, 870 (1986).
[28] C. Kittel and H. Kroemer, in *Thermal Physics*, 2nd ed. (Freeman, New York, 1980).
[29] K. M. van Vliet, Appl. Opt. **6**, 1145 (1967).
[30] J. C. Mather, Appl. Opt. **21**, 1125 (1982).
[31] E. Jakeman and E. R. Pike, J. Phys. A (Proc. Phys. Soc.) **1**, 128 (1968).
[32] E. Jakeman, C. J. Oliver, and E. R. Pike, J. Phys. A (Proc. Phys. Soc.) **1**, 406 (1968).
[33] F. J. Low and A. R. Hoffman, Appl. Opt. **2**, 649 (1963).
[34] J. C. Mather, Appl. Opt. **24**, 1407 (1985).
[35] N. Coron, Infrared Phys. **16**, 411 (1976).
[36] A. L. Efros and B. I. Shklovskii, in *Electronic Properties of Doped Semiconductors* (Springer, New York, 1984), p. 202.
[37] J. W. Beeman and E. E. Haller (unpublished).
[38] Kohei Itoh, W. L. Hansen, W. L., E. E. Haller, J. W. Farmer, V. I. Ozhogin, A. Rudnev, and A. Tikhomirov, J. Mater. Res. **8**, 1341 (1993).
[39] T. W. Kenny, P. L. Richards, I. S. Park, E. E. Haller, and J. W. Beeman, Phys. Rev. B **39**, 8476 (1989).
[40] S. M. Grannan, A. E. Lange, E. E., Haller, and J. W. Beeman, Phys. Rev. B **45**, 4516 (1992).
[41] F. J. Low (private communication, 1991).
[42] M. W. Werner, J. H. Elias, D. Y. Gezari, M. G. Hauser, and W. E. Westbrook, Astrophys. J. **199**, L185 (1975).
[43] N. S. Nishioka, P. L. Richards, and D. P. Woody, Appl. Opt. **19**, 1562 (1978).
[44] B. Carli and D. Iorio-Fili, J. Opt. Soc. Am. **71**, 1020 (1981).
[45] M. Dragovan and S. H. Moseley, Appl. Opt. **23**, 654 (1984).
[46] M. J. E. Golay, Rev. Sci. Instrum. **20**, 816 (1949).
[47] L. Harris, J. Opt. Soc. Am. **51**, 80 (1961).
[48] I. Hoffman and D. Stroud, Phys. Rev. B **43**, 9965 (1991).
[49] A. T. Serlemitsos, Proc. SPIE **973**, 314 (1988).
[50] D. C. Alsop, C. Inman, A. E. Lange, and T. Wilbanks, Appl. Opt. **31**, 6610 (1992).
[51] A. E. Lange, S. Hayakawa, T. Matsumoto, H. Matsuo, H. Murakami, P. L. Richards, and S. Sato, Appl. Opt. **26**, 401 (1987).
[52] A. C. Clapp, C. Hagmann, A. E. Lange, P. L. Richards, S. T. Tanaka, and P. T. Timbie (unpublished 1992).
[53] D. Miller, P. L. Richards, S. Etemad, A. Inam, T. Venkatesan, B. Dutta, X. D. Wu, C. B. Eom, T. H. Geballe, N. Newman, and B. F. Cole, Phys. Rev. B **47**, 8076 (1993).
[54] S. H. Moseley, J. C. Mather, and D. McCammon, J. Appl. Phys. **56**, 1257 (1984).
[55] P. T. Timbie, S. H. Moseley, and P. L. Richards (unpublished, 1990).
[56] R. Winston, J. Opt. Soc. Am. **60**, 245 (1970).
[57] R. H. Hildebrand, Opt. Eng. **25**, 323 (1986).
[58] J. A. Murphey and R. Padman, Infrared Phys. **31**, 291 (1991).
[59] D. E. Williamson, J. Opt. Soc. Am. **42**, 712 (1952).
[60] M. Fischer, D. C. Alsop, E. S. Cheng, A. C. Clapp, D. A. Cottingham, J. O. Gunderson, T. C. Koch, E. Kreysa, P. R. Meinhold, A. E. Lange, P. M. Lubin, P. L. Richards, and G. F. Smoot, Astrophys. J. **388**, 242 (1992).
[61] J. C. Mather, IEEE Trans. Antennas Prop. **AP-29**, 967 (1981).
[62] C. R. Cunningham and W. K. Gear, Proc. SPIE **1235**, 515 (1990).
[63] W. E. Lamb, Jr., Phys. Rev. **70**, 308 (1946).
[64] E. Kreysa (unpublished, 1992).
[65] J. C. Peterson and M. A. Goldman, Int. J. Infrared Millimeter Waves **9**, 55 (1988).
[66] F. M. Rieke, A. E. Lange, J. W. Beeman, and E. E. Haller, IEEE Trans. Nucl. Sci. **36**, 946 (1989).
[67] M. Devlin, A. E. Lange, and T. Wilbanks, Nuclear Science Symposium, Santa Fe, NM, November 1991 (unpublished).
[68] E. N. Glezer, A. E. Lange, T. Wilbanks, Appl. Opt. **31**, 9214 (1992).
[69] D. McDonald, Appl. Phys. Lett. **50**, 775 (1987).
[70] J. Clarke, in *Superconducting Electronics*, NATO ASI Series Vol. 59 edited by H. Weinstock and M. Nisenoff (Springer, Berlin, 1989), pp. 88–147.
[71] M. Nahum and P. L. Richards, IEEE Trans. Magn. **MAG-27**, 2484 (1991).
[72] J. Mees, M. Nahum, and P. L. Richards, Appl. Phys. Lett. **59**, 2329 (1991).
[73] T.-L. Hwang, S. E. Schwartz, and D. B. Rutledge, Appl. Phys. Lett. **34**, 773 (1979).
[74] D. B. Rutledge, D. P. Neikirk, and D. P. Kasilingam, in *Infrared and Millimeter Waves*, edited by K. J. Button (Academic, New York, 1983), Vol. 10, pp. 1–90.
[75] E. N. Grossman, J. E. Sauvageau, and D. G. McDonald, Appl. Phys. Lett. **59**, 3225 (1991).
[76] J. G. Henston, J. M. Lewis, S. M. Wentworth, D. P. Neikirk, Microsc. Opt. Technol. Lett. **4**, 15 (1991).
[77] H. Ekström, S. Gearhart, P. R. Acharya, H. Dave, G. Rebeitz, S. Jacobsson, E. Kollberg, and G. Chin, Proceedings of the Third International Symposium on Space THz Technologies, Ann Arbor, Michigan, 1992 (unpublished).
[78] M. Nahum, C. A. Mears, and P. L. Richards, IEEE Trans. Appl. Supercond. **3**, 2124 (1993).
[79] M. Nahum and J. M. Martinis, Appl. Phys. Lett. **63**, 3075 (1993).
[80] P. L. Richards, J. Clarke, R. Leoni, P. H. Lerch, S. Verghese, M. R. Beasley, T. H. Geballe, R. H. Hammond, P. Rosenthal, and S. R. Spielman, Appl. Phys. Lett. **54**, 283 (1989).
[81] S. Verghese, P. L. Richards, K. Char, S. A. Sachtjen, IEEE Trans. Magn. **MAG-27**, 3077 (1991).
[82] S. Verghese, P. L. Richards, S. A. Sachtjen, and K. Char, J. Appl. Phys. **24**, 4251 (1993).
[83] J. C. Brasunas, S. H. Moseley, B. Lakew, R. H. Ono, D. G. McDonald, J. A. Beall, and J. E. Sauvageau, J. Appl. Phys. **66**, 4551 (1989).
[84] J. C. Brasunas, S. H. Moseley, B. Lakew, R. H. Ono, D. G. McDonald, J. A. Beall, and J. E. Sauvageau, SPIE Proc. **1292**, 155 (1990).
[85] T. G. Stratton, B. E. Cole, P. W. Kruse, R. A. Wood, K. Beauchamp, T. F. Want, B. Johnson, and A. M. Goldman, Appl. Phys. Lett. **57**, 99 (1990).
[86] B. R. Johnson, T. Ohnstein, C. J. Han, R. Higashi, P. W. Kruse, R. A. Wood, H. Marsh, and S. B. Dunham, IEEE Trans. Appl. Supercond. **3**, 2856 (1993).
[87] S. Verghese, P. L. Richards, K. Char, D. K. Fork, and T. H. Geballe, J. Appl. Phys. **71**, 2491 (1992).
[88] Q. Hu and P. L. Richards, Appl. Phys. Lett. **55**, 2444 (1989).
[89] M. Nahum, Q. Hu, and P. L. Richards, IEEE Trans. Magn. **MAG-27**, 3081 (1991).
[90] M. Nahum, S. Verghese, P. L. Richards, and K. Char, Appl. Phys. Lett. **59**, 2034 (1991).
[91] G. L. Carr, M. Quijada, D. B. Tanner, C. J. Hirschmugl, G. P. Williams, S. Etemad, B. Dutta, F. DeRosa, A. Inam, T. Venkatesan, and X. Xi, Appl. Phys. Lett. **57**, 2725 (1990).
[92] C. Kittel, in *Introduction to Solid State Physics*, 6th ed. (Wiley, New York, 1986).
[93] T. W. Kenny and P. L. Richards, Phys. Rev. Lett. **64**, 2386 (1990).
[94] N. E. Phillips, CRC Crit. Rev. Solid State Sci. **2**, 467 (1971).
[95] O. U. Lounasmaa, in *Experimental Principles and Methods Below 1 K* (Academic, London, 1974).
[96] E. G. Childs, L. J. Ericks, and R. L. Powell, *Thermal Conductivity of Solids at Room Temperature and Below* (National Bureau of Standards, Washington, DC, 1973), Monograph 131.